

Identification of 2,6-Disubstituted-3-imidazo[4,5-*b*]pyridines as Therapeutic Agents for Dysferlinopathies through Phenotypic Screening on Patient-Derived iPSCs

HiroYuki Takada, Akira Kaieda, Michiko Tawada, Tomoko Nagino, Katsunori Sasa, Tatsuo Oikawa, Akiko Oki, Tomoya Sameshima, Kazumasa Miyamoto, Makoto Miyamoto, Yuko Kokubu, Ryuichi Tozawa, Hidetoshi Sakurai, and Bunnai Saito

J. Med. Chem., **Just Accepted Manuscript** • DOI: 10.1021/acs.jmedchem.9b01100 • Publication Date (Web): 24 Sep 2019

Downloaded from pubs.acs.org on September 25, 2019

Just Accepted

"Just Accepted" manuscripts have been peer-reviewed and accepted for publication. They are posted online prior to technical editing, formatting for publication and author proofing. The American Chemical Society provides "Just Accepted" as a service to the research community to expedite the dissemination of scientific material as soon as possible after acceptance. "Just Accepted" manuscripts appear in full in PDF format accompanied by an HTML abstract. "Just Accepted" manuscripts have been fully peer reviewed, but should not be considered the official version of record. They are citable by the Digital Object Identifier (DOI®). "Just Accepted" is an optional service offered to authors. Therefore, the "Just Accepted" Web site may not include all articles that will be published in the journal. After a manuscript is technically edited and formatted, it will be removed from the "Just Accepted" Web site and published as an ASAP article. Note that technical editing may introduce minor changes to the manuscript text and/or graphics which could affect content, and all legal disclaimers and ethical guidelines that apply to the journal pertain. ACS cannot be held responsible for errors or consequences arising from the use of information contained in these "Just Accepted" manuscripts.

Identification of 2,6-Disubstituted-3*H*-imidazo[4,5-*b*]pyridines as Therapeutic Agents for Dysferlinopathies through Phenotypic Screening on Patient-Derived iPSCs

Hiroyuki Takada,^{,†} Akira Kaieda,[†] Michiko Tawada,[†] Tomoko Nagino,[‡] Katsunori Sasa,[‡] Tatsuo Oikawa,[‡] Akiko Oki,[†] Tomoya Sameshima,[†] Kazumasa Miyamoto,[†] Makoto Miyamoto,[†] Yuko Kokubu,[§] Ryuichi Tozawa,[‡] Hidetoshi Sakurai,[§] and Bunnai Saito[†]*

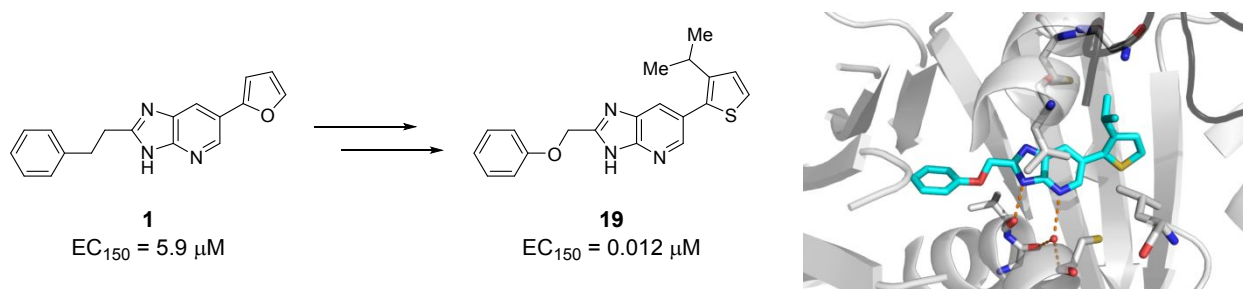
[†]Research, Takeda Pharmaceutical Company Limited, 26-1, Muraoka-Higashi 2-chome, Fujisawa, Kanagawa 251-8555, Japan

[‡]T-CiRA Discovery, Takeda Pharmaceutical Company Limited, 26-1, Muraoka-Higashi 2-chome, Fujisawa, Kanagawa 251-8555, Japan

[§]Center for iPS Cell Research and Application, Kyoto University, 53 Kawahara-cho, Shogoin, Sakyo-ku, Kyoto 606-8507, Japan.

ABSTRACT:

Dysferlinopathies, which are muscular diseases caused by mutations in dysferlin gene, remain serious medical problems due to the lack of therapeutic agents. Herein, we report the design, synthesis, and structure-activity relationships of a 2,6-disubstituted-3*H*-imidazo[4,5-*b*]pyridine series, which was identified from the phenotypic screening of chemicals that increase the level of dysferlin in myocytes differentiated from patient-derived induced pluripotent stem cells (iPSCs). Optimization studies with cell-based phenotypic assay led to the identification of a highly potent compound **19** with dysferlin elevation effects at double-digit nanomolar concentrations. In addition, the molecular target of our chemical series was identified as tubulin, through a tubulin polymerization assay and a competitive binding assay using a photoaffinity labeling probe.



Key words: small molecule, phenotypic screening, induced pluripotent stem cells (iPSCs), dysferlinopathy, dysferlin (DYSF), tubulin, photoaffinity labeling (PAL) probe, target identification

INTRODUCTION

Cell-based phenotypic screening is an attractive drug discovery approach because it does not require an established biological knowledge of molecular targets, and it leads to the discovery of novel druggable targets and therapeutic agents.^{1,2} In particular, phenotypic screening using patient-derived induced pluripotent stem cells (iPSCs) is expected to be one of the most disease-relevant evaluation systems.³⁻⁶ Dysferlinopathies are autosomal recessive muscular disorders that are caused by mutations in the dysferlin gene.^{7,8} Dysferlin is dominantly expressed in skeletal or cardiac muscles and plays an essential role in the repair of damaged and disrupted plasma membranes.⁹⁻¹¹ The loss or reduction of dysferlin results in the weakening of muscles as the muscle membrane is not restored sufficiently. Dysferlinopathies are clinically categorized into at least three phenotypes based on the initial pattern of muscle weakness: limb girdle muscular dystrophy 2B (LGMD2B), Miyoshi myopathy (MM), and distal myopathy with anterior tibial onset (DMAT). Currently, there is no effective treatment for dysferlinopathies; therefore, the development of novel therapeutic agents is highly desired.

Many types of dysferlin mutations have been reported, and it is evident that dysferlin level in human fibroblasts with the c.2997G>T (p.W999C) missense mutation is much lower than that in normal human fibroblasts.¹² Additionally, treatment with a proteasomal inhibitor, MG-132, increased the level of p.W999C mutated dysferlin protein, and the membrane blebbing level was

also restored depending on the increase in the level of mutated dysferlin. Therefore, it is suggested that p.W999C mutated dysferlin protein possesses membrane resealing function. Indeed, a clinical study reported that patients with the homozygous c.2997G>T mutation had late onset of dysferlinopathies relative to those with the heterozygous c.2997G>T mutation.¹³ These observations indicate that an increase in the level of p.W999C mutated dysferlin protein could alleviate the symptoms of dysferlinopathies. Moreover, we previously developed a rapid, efficient, and reproducible method to differentiate iPSCs into mature myocytes, and we demonstrated its application in a disease model of MM.¹⁴ This method enabled us to establish an assay system to screen chemicals that could increase the dysferlin level in myocytes differentiated from MM patient-derived iPSCs.¹⁵ The pilot screening of 622 commercially available compounds identified nocodazole, a tubulin inhibitor, as a hit compound, which was found to restore membrane resealing function.

Following the pilot screening, we carried out a more extensive high-throughput screening of small molecules to find more potent and drug-like compounds. From a screen of structurally diverse and drug-like small molecules (ca. 6400), we identified 2,6-disubstituted-3*H*-imidazo[4,5-*b*]pyridine **1** as a hit compound, which showed dysferlin elevation effects in a dose-dependent manner. Compound **1** and its derivatives were originally derived in Takeda's legacy project, where these compounds exhibited the growth inhibition of

HER2-positive cell lines such as SK-BR-3 and BT-474; however, their molecular target remains unknown.¹⁶ In the present study, we describe the structure-activity relationships (SAR) of 2,6-disubstituted-3*H*-imidazo[4,5-*b*]pyridines and our efforts on the target deconvolution of our chemical series.

RESULTS AND DISCUSSION

In the dysferlin elevation assay,¹⁵ the threshold value for detecting an increase in the dysferlin level was set as median + 3 standard deviations of vehicle controls, which converged to slightly less than 1.5-fold relative to the median value of vehicle controls. Therefore, we defined the indicator of potency, EC₁₅₀, as a compound concentration at which the dysferlin level is increased by 1.5-fold. As a result of the high throughput screening, we identified a hit compound **1**, which exhibited an EC₁₅₀ value of 5.9 μ M and acceptable physicochemical properties such as solubility and membrane permeability. As our assay was a cell-based phenotypic screening, it is noteworthy that compound **1** did not show any cytotoxic effect on HepG2 cells even at 100 μ M. Thus, we executed SAR studies in order to understand which features are crucial for cellular activity and identify highly potent compounds. The SAR information is also required for target identification approaches such as chemical proteomics or correlation analysis with target-based assay results¹⁷,¹⁸; for example, it is crucial for the preparation of chemical probes to clarify which part of the

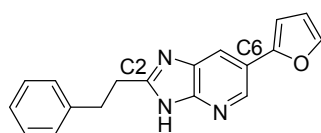
compound turns toward the solvent region to attach a linker motif without disrupting the potency.

In developing the cell-based SAR using the dysferlin elevation assay, the structure of compound

1 was divided into three structural units: 1) C-2 substituents on imidazopyridine; 2) C-6 aryl

groups on imidazopyridine; 3) imidazopyridine core scaffold. We carried out systematic

modifications of each structural unit and evaluated the effects on the dysferlin level.



Compound 1

Cellular activity: $EC_{150} = 5.9 \mu M$

Permeability: 332 nm/sec

Solubility: 6.4 $\mu g/mL$

Cytotoxicity: $IC_{50} > 100 \mu M$

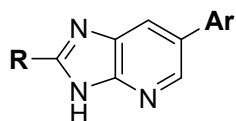
Figure 1. Structure of hit compound **1**.

First, the effects of C-2 substituents on cellular activity were investigated. Replacing the phenethyl group at C-2 with a phenyl (**2**) or benzyl (**3**) group resulted in the loss of cellular activity. To confirm the tolerability of substitution on the terminal phenyl ring, a chlorine atom was introduced into the *ortho*-, *meta*- and *para*-position, respectively. Among these, *para*-substituted **6** showed a potency comparable to **1**, whereas *ortho*- (**4**) or *meta*- (**5**) substituted compounds showed reduced potency. The *para*-substitution was tolerated, and hence, a variety of *para*-substitution was explored. Consequently, a fluorophenethyl group (**9**) increased potency by

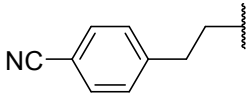
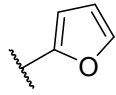
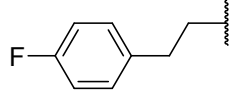
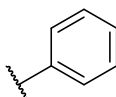
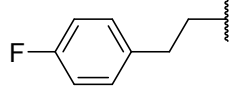
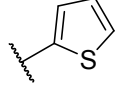
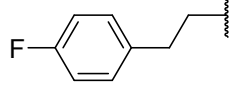
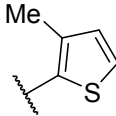
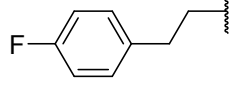
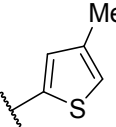
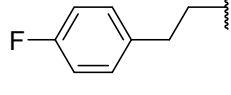
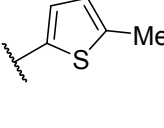
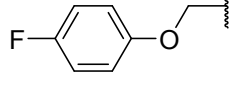
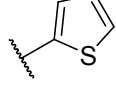
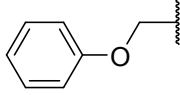
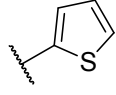
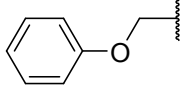
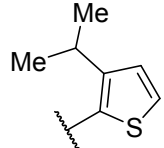
approximately 6-fold compared to hit compound **1**. In contrast, an electron donating methyl (**7**) or methoxy group (**8**) and an electron withdrawing trifluoromethyl (**10**) or cyano group (**11**) resulted in a loss in potency, suggesting the size limitations of the binding pocket around the terminal phenyl ring.

With the potent compound **9** in hand, we explored the aryl group at C-6. While replacing the furan ring with a benzene ring (**12**) hardly affected cellular activity, compound **13** containing a thiophene ring exhibited an approximately 7-fold increase in potency as compared to **9**. The addition of a methyl group into the 3-position of the thiophene ring (**14**) was tolerated; however, the substitution at the 4 or 5-position (**15** or **16**) resulted in a reduction of cellular activity. As in compound **17**, the ether-linked C-2 group resulted in an approximately 2-fold increase in potency compared to the corresponding carbon-linked analogue **13**. Surprisingly, the elimination of the fluorine atom on the phenyl ring of compound **17** slightly enhanced the potency as in compound **18**. In addition, it should be noted that compound **18** exhibited no cytotoxic effect as with the case of hit compound **1**. Given that the 3-position methyl group on the thiophene ring was tolerated as in **14**, a bulkier isopropyl group was introduced into the thiophene ring of compound **18**, which led to an approximately 3-fold increase in potency (**19**).

Table 1. Structure-Activity Relationships of C-2 and C-6 Groups



Compound	R	Ar	EC ₁₅₀ (μM) ^a
1			5.9 (3.3–10)
2			>10
3			>10
4			>10
5			>10
6			4.3 (2.4–7.6)
7			>10
8			>10
9			1.0 (0.45–2.3)
10			>10

11			>10
12			1.3 (0.51–3.2)
13			0.15 (0.064–0.33)
14			0.11 (0.080–0.25)
15			1.9 (0.75–5.0)
16			6.3 (1.5–26)
17			0.067 (0.037–0.12)
18			0.039 (0.017–0.087)
19			0.012 (0.0058–0.023)

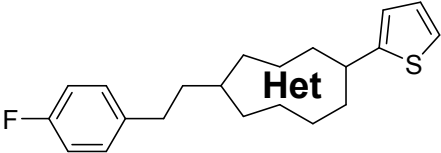
^a n = 8, 95 % confidence intervals shown in parentheses.

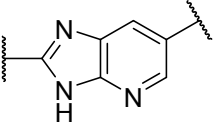
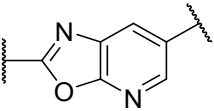
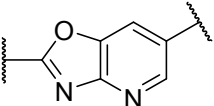
Next, we investigated the role of the imidazopyridine core in cellular activity.

Oxazolo[4,5-*b*]pyridines **20** and **21** exhibited a considerable loss in potency, indicating that the

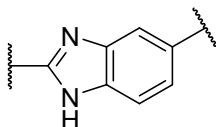
NH group of the imidazole ring might contribute to cellular activity by the formation of a hydrogen bond with the target protein. Similarly, upon the removal of the nitrogen atom of the pyridine ring, the resultant benzimidazole **22** did not exhibit a dysferlin elevation effect even at 10 μ M. Furthermore, the introduction of a methyl group adjacent to the pyridine nitrogen resulted in the loss of cellular activity as in **23**. These results implied that the pyridine nitrogen possibly made a hydrogen bond with the target protein, thereby contributing to cellular activity. In contrast, the introduction of a methyl group at the 7-position of imidazopyridine ring was relatively tolerated, as in **24**. As a result, 3*H*-imidazo[4,5-*b*]pyridine was found to be the optimal core structure for cellular activity.

Table 2. Structure-Activity Relationships of the Center Ring



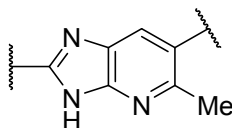
Compound	Het	EC ₁₅₀ (μ M) ^a
13		0.15 (0.064–0.33)
20		>10
21		>10

22



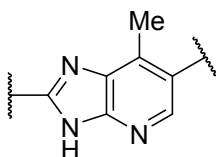
>10

23



>10

24



0.37 (0.17–0.82)

^a n = 8, 95 % confidence intervals shown in parentheses.

Furthermore, we sought to elucidate the plausible target of the chemical series. We previously reported that the tubulin inhibitors, nocodazole and colchicine¹⁹, increased the level of dysferlin in our dysferlin elevation assay.¹⁵ Accordingly, we proposed that the cellular activity of the 2,6-disubstituted-3*H*-imidazo[4,5-*b*]pyridine series would be mediated by the inhibition of tubulin polymerization. The inhibitory effects of several analogues on tubulin polymerization were evaluated in HepG2 cells to determine if they are correlated with dysferlin elevation effects on iPSC-derived myocytes (for the structure of measured compounds, see **Table S1**, Supporting Information). As hypothesized, the correlation plot suggests that the inhibition of tubulin polymerization caused the elevation of dysferlin in the chemical series (**Figure 2**). It is worth noting that the compound series did not exhibit inhibitory activities against kinases through competitive binding assays, although 3*H*-imidazo[4,5-*b*]pyridine is a typical hinge binder.

(Figure S1, Supporting Information)

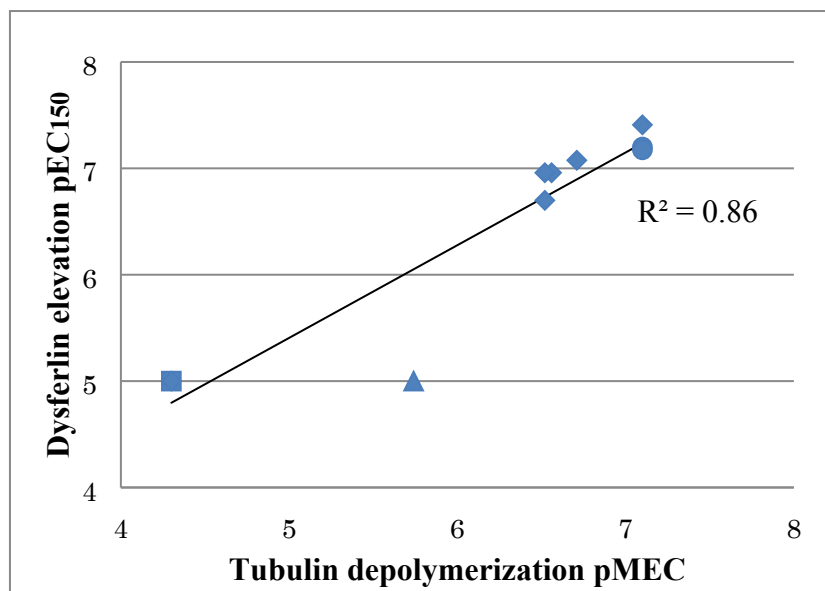


Figure 2. Correlation plot of pEC_{150} with tubulin depolymerization pMEC. MEC, minimal effective concentration; R, correlation coefficient. The EC_{150} value of compounds described as square or triangle is $>10 \mu M$. The MEC value of compounds described as circle or square is $<0.080 \mu M$ or $>50 \mu M$, respectively.

Encouraged by these results, we performed docking studies in order to further elucidate the binding modes of the chemical series with tubulin molecules. It is reported that nocodazole binds to the interface of alpha/beta-tubulin hetero dimers, which is known as the colchicine binding site.²⁰ Nocodazole contains an imidazole ring, which is an essential moiety for cellular activity in our chemical series, and hence, we thought nocodazole and our chemical series might bind to the

common binding site (Figure **3a**). We conducted the docking calculation for compound **19** based on the X-ray co-crystal structure of nocodazole with tubulin (PDB code: 5CA1) (Figure **3b-c**). Our docking analysis suggested that the NH-group of the imidazole ring made a hydrogen bond with the back bone oxygen atom of Val236 of beta-tubulin. The loss in potency of oxazolo[4,5-*b*]pyridines **20** and **21** should be attributed to the absence of this interaction. In addition, the nitrogen atom of the pyridine ring formed a water-mediated hydrogen bond with Gly235 and Cys239 of beta-tubulin. In the X-ray co-crystal structure of nocodazole, the water molecule tightly binds to Gly235 and Cys239, and the water-mediated interaction is formed by the carbonyl group on the thiophene ring (Figure **3d**).²⁰ These results are consistent with the observation that benzimidazole **22** without the nitrogen atom had a considerable loss in potency. The isopropyl group on the thiophene ring occupies the hydrophobic region consisting of Leu246, Leu253, Asn256, and Met257 of beta-tubulin. This hydrophobic interaction is considered to contribute to the high potency of compound **19**. Generally, our docking model explains the SAR of the chemical series.

(a)

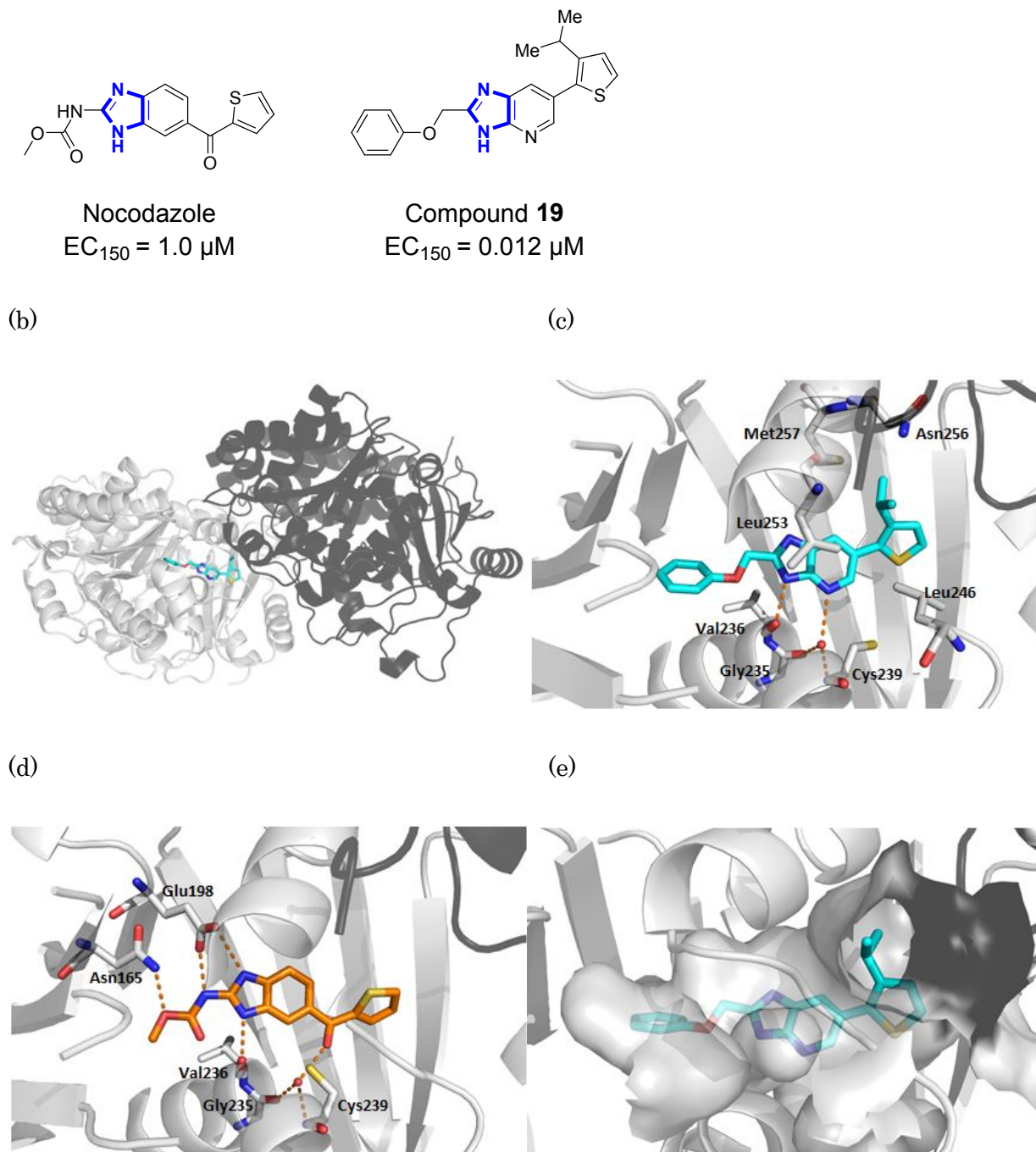


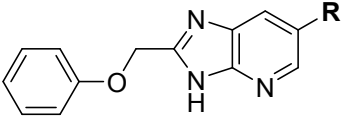
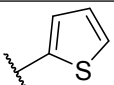
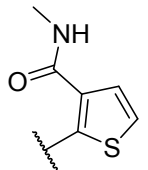
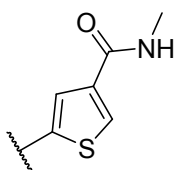
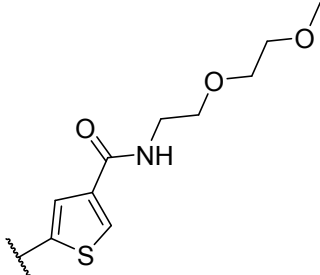
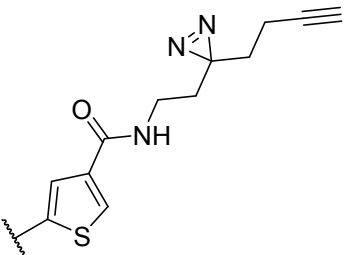
Figure 3. (a) Structure and cellular activity of nocodazole and compound **19**. (b) Docking model of **19** with an alpha/beta-tubulin hetero dimer. Compound **19** is light blue, alpha-tubulin is black, and beta-tubulin is grey. (c) The binding site of **19**. Residues that form hydrogen bonds or hydrophobic

interactions with **19** are shown as sticks and are labeled. (d) X-ray co-crystal of nocodazole with tubulin (PDB code: 5CA1). Residues that form hydrogen bonds with the ligand are shown as sticks and are labeled. (e) Surface of residues within 4.0 Å of **19**.

Our docking model was found to be consistent with SAR, and hence, we tried to confirm the direct binding between our compounds and tubulins using a photoaffinity labeling (PAL) probe, which covalently binds to its target protein after ultraviolet irradiation.²¹ Our docking model indicated that there was a long and narrow cavity exposed to the solvent region around the 3- and 4-positions of the thiophene ring, suggesting that a chemical probe linker could be attached without disrupting the binding affinity to tubulins (**Figure 3e**). Thus, we introduced a linker motif into the thiophene ring of compound **18** and evaluated its effect on the level of dysferlin. First, an amide group was introduced because it is synthetically feasible to extend various linker parts by amide coupling. Unlike in the case of the methyl or isopropyl group, a methanamide group at the 3-position of the thiophene ring resulted in a considerable loss of cellular activity (**25**). In contrast, compound **26** containing a methanamide group at the 4-position sustained high potency. Furthermore, a 2-(2-methoxyethoxy)ethanamide group was also tolerated, as in compound **27**, suggesting that the terminal alkoxy chain should turn toward the solvent region. Based on these results, we synthesized a PAL probe **28**, containing a photo-reactive diazirine group and an

alkyne tag, which exhibited cellular activity at submicromolar concentrations.

Table 3. Preparation of PAL probe 28

		
Compound	R	EC ₁₅₀ (μM) ^a
18		0.039 (0.017–0.087)
25		>10
26		0.11 (0.038–0.31)
27		0.40 (0.096–1.7)
28		0.37 (0.20–0.69)

^a n = 8, 95 % confidence intervals shown in parentheses.

With probe **28** and purified tubulins, a competitive binding assay was carried out. Commercially available porcine brain tubulins were incubated with **28** after pre-incubation with or without competitive compounds, followed by ultraviolet irradiation for crosslinking between **28** and tubulins. Subsequently, the crosslinked tubulins were labeled with a fluorescent dye, tetramethylrhodamine (TAMRA), by alkyne-azide click-reaction. The tubulins were separated by SDS-PAGE, and the images for fluorescently labeled tubulins and total tubulins were captured (**Figure 4**). The fluorescently labeled tubulins were clearly observed without competitive compounds, suggesting that probe **28** was effectively bound to the tubulins. In addition, the same fluorescent band was not detected in the case where the porcine brain tubulins were pre-incubated with compound **18** ($EC_{150} = 0.039 \mu\text{M}$) before the treatment with **28**, whereas pre-incubation with compound **21** ($EC_{150} > 10 \mu\text{M}$) hardly affected the fluorescent labeling. Furthermore, competitive inhibition was observed when the porcine tubulins were pre-treated with colchicine binding site inhibitors such as colchicine and nocodazole. In contrast, pre-incubation with vinblastine and paclitaxel, which are known to bind to other binding sites¹⁹, did not inhibit the binding of probe **28**. These results demonstrated that our chemical series increased the dysferlin level because of tubulin depolymerization caused by direct binding to the colchicine binding site of tubulins.

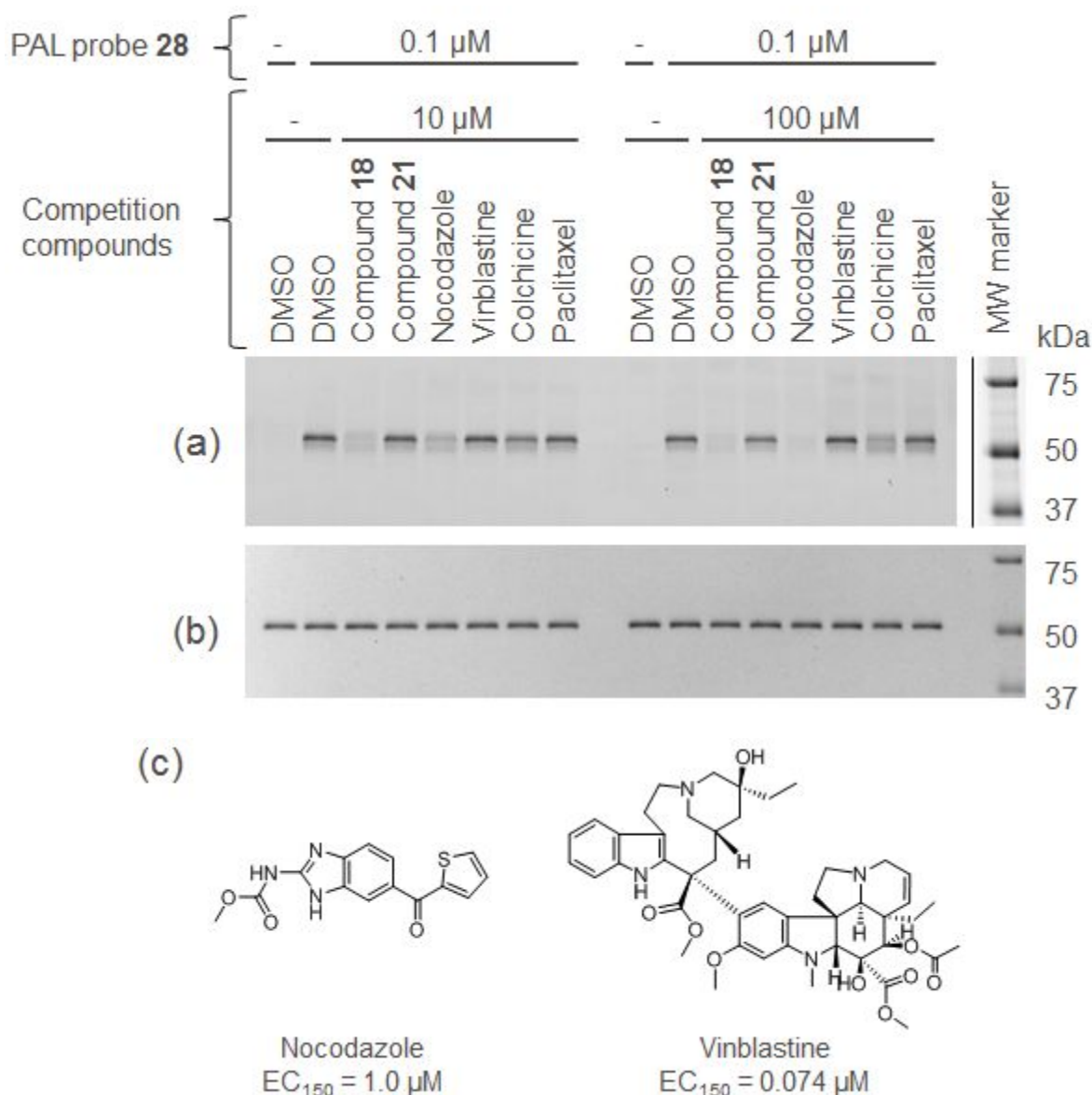


Figure 4. Image of SDS-PAGE for PAL probe-labeled tubulins. The tubulins were labeled with PAL probe 28 after pre-incubation with non-labeled active or inactive compound (compound 18 or 21, respectively) or known tubulin binders. PAL probe 28, which has an acetylene group, was probed with TAMRA-azide by click reaction. (a) The samples were analyzed by SDS-PAGE, and the fluorescence images were captured to detect the PAL-probe-labeled tubulins. (b) Subsequently, the gel was stained with

Coomassie brilliant blue to visualize the total tubulin. (c) Structure and cellular activity of nocodazole and vinblastine.

CONCLUSIONS

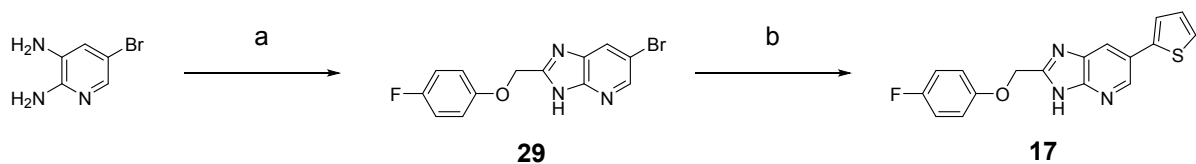
In summary, we investigated the SAR of a 2,6-disubstituted-3*H*-imidazo[4,5-*b*]pyridine series using a cell-based phenotypic screening in myocytes differentiated from MM patient-derived iPSCs to identify compound **19**, which exhibited dysferlin elevation effects at double-digit nanomolar concentrations. The cellular activity of this chemical series correlated with their inhibitory activity on tubulin polymerization. The competitive binding assay using purified tubulins demonstrated that PAL probe **28** covalently bound to tubulins and it was competitively inhibited by the active compound **18** or the colchicine binding site inhibitors, colchicine and nocodazole. These observations indicated that 2,6-disubstituted-3*H*-imidazo[4,5-*b*]pyridines increased the level of dysferlin through the inhibition of tubulin polymerization, mediated by direct binding of the compounds to the colchicine binding site of tubulins. These results are consistent with our previous work, where we demonstrated that nocodazole increased dysferlin protein levels and improved the membrane resealing function. Considering that misfolded proteins are transported along microtubules to form autophagosome in autophagy system, it is suggested that the upregulation of dysferlin should be attributed to the blockage of the

1
2
3
4 microtubule-dependent autophagy which might contribute to degradation of mutated dysferlin
5
6
7 protein. Indeed, upon the treatment of nocodazole, the accumulation of p62 and LC3 II were
8
9
10 observed, which indicated disruption of autophagy.¹⁵ Further investigation for the elucidation of
11
12
13 the detailed mechanism of action is underway. On the other hand, due to potential adverse effects
14
15
16 of microtubule disruption, such as cell cycle arrest, further optimization of the chemical series
17
18
19 was discontinued.²² However, we strongly believe that compound **19** can be used as a tool
20
21
22 compound to elucidate the detailed mechanism of action. Thus, it can contribute to the discovery
23
24
25 of druggable molecular targets and ultimately novel therapeutic agents for dysferlinopathies.
26
27
28
29
30

31 CHEMISTRY

32
33
34 The synthesis of compound **17** is outlined in **Scheme 1**. Commercially available
35
36
37 5-bromo-2,3-diamino-pyridine was coupled with 2-(4-fluorophenoxy)acetic acid in the presence
38
39
40 of 2-(7-aza-1*H*-benzotriazole-1-yl)-1,1,3,3-tetramethyluronium hexafluorophosphate (HATU)
41
42
43 and *N,N*-diisopropylethylamine (DIPEA), followed by intramolecular condensation in the acidic
44
45
46 conditions to afford imidazopyridine intermediate **29**. The intermediate **29** was converted to
47
48
49 compound **17** by Suzuki-Miyaura coupling with thiophen-2-ylboronic acid. Compounds **1-19** and
50
51
52 **22-25** were prepared in a manner similar to **Scheme 1**.
53
54
55
56
57
58
59
60

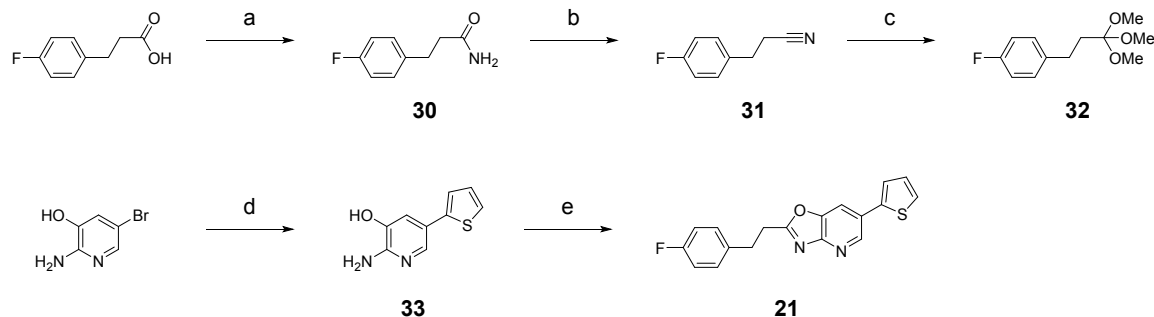
Scheme 1. Synthesis of compound 17^a



^aReagents and conditions: (a) (i) HATU, DIPEA, 2-(4-fluorophenoxy)acetic acid, DMF; (ii) AcOH, reflux, 70 % (2 steps); (b) Pd(Amphos)Cl₂, Na₂CO₃, thiophen-2-ylboronic acid, DME, water, microwave 120 °C, 17 %.

Compound **21** was prepared according to **Scheme 2**. Commercially available 3-(4-fluorophenyl)propanoic acid was converted to carboxamide **30**, and the following dehydration afforded the corresponding nitrile **31**. Compound **31** was reacted with methanol under acidic conditions to give orthoester **32**, followed by condensation with aminohydroxypridine **33** prepared from commercially available 2-amino-5-bromopyridin-3-ol via Suzuki-Miyaura coupling to afford compound **21**. Compound **20**, a regioisomer of **21**, was prepared in a manner similar to **Scheme 2**.

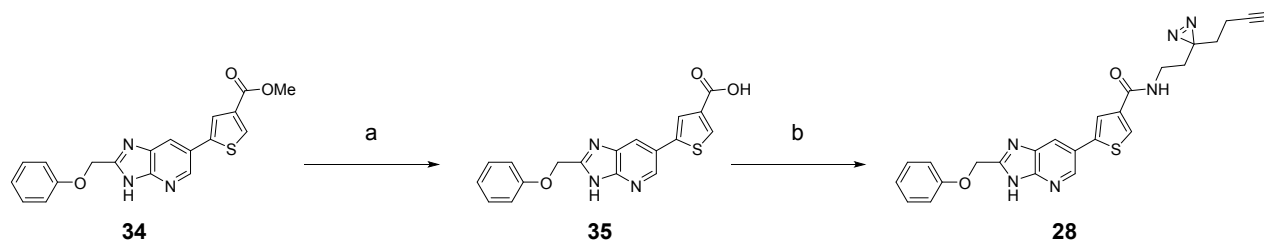
Scheme 2. Synthesis of compound 21^a



^aReagents and conditions: (a) (i) (COCl)₂, DMF (cat), CHCl₃; (ii) NH₃, CHCl₃, 0 °C-RT, 76 % (2 steps); (b) trifluoroacetic anhydride, 90 %; (c) (i) HCl gas, MeOH, Et₂O, 0 °C-4 °C; (ii) MeOH, hexane; (d) PdCl₂(PPh₃)₂, Na₂CO₃, thiophen-2-ylboronic acid, 1,4-dioxane, water, 110 °C, 59 %; (e) AcOH, toluene, reflux, 73 %.

The synthesis of PAL probe **28** is outlined in **Scheme 3**. The intermediate **34** was prepared according to **Scheme 1**, and then hydrolyzed to give carboxylic acid **35**. Compound **28** was obtained through amide coupling between carboxylic acid **35** and 2-(3-(but-3-yn-1-yl)-3*H*-diazirin-3-yl)ethan-1-amine. Compound **26** and **27** were prepared in a manner similar to **Scheme 3**.

Scheme 3. Synthesis of compound 28^a



^aReagents and conditions: (a) NaOH aq., MeOH, THF, 86 %; (b) HATU, DIPEA, 2-(3-(but-3-yn-1-yl)-3H-diazirin-3-yl)ethan-1-amine, DMF, 65 %.

EXPERIMENTAL SECTION

General Chemistry Information.

¹H NMR spectra were recorded on Bruker AVANCE-300, 400, or 500 (300, 400, or 500 MHz).

Chemical shifts are given in parts per million (ppm) with tetramethylsilane as an internal

standard. Abbreviations used are as follows: s = singlet, d = doublet, t = triplet, q = quartet, m =

multiplet, dd = doublet of doublets, td = triplet of doublets, brs = broad singlet. Coupling

constants (*J* values) are given in hertz (Hz). The acidic protons were not frequently observed in

¹H NMR spectra. Low-resolution mass spectra (MS) were acquired using an Agilent LC/MS

system (Agilent1200SL/Agilent6130MS) or Shimadzu UFLC/MS (Prominence UFLC high

pressure gradient system/LCMS-2020) operating in an electrosprayionization mode (ESI+). The

column used was an L-column 2 ODS (3.0 mm × 50 mm I.D., 3 μm, CERI) with a temperature of

40 °C and a flow rate of 1.2 or 1.5 mL/min. Condition 1: Mobile phases A and B under an acidic

condition were 0.05% TFA in water and 0.05% TFA in MeCN, respectively. The ratio of mobile phase B was increased linearly from 5 to 90% over 0.9 min, 90% over the next 1.1 min.

Condition 2: Mobile phases A and B under a neutral condition were a mixture of 5 mM AcONH₄ and MeCN (9/1, v/v) and a mixture of 5 mM AcONH₄ and MeCN (1/9, v/v), respectively. The ratio of mobile phase B was increased linearly from 5 to 90% over 0.9 min, 90% over the next 1.1 min. Chemical intermediates were characterized by ¹H NMR and/or mass spectral data.

Unless otherwise stated, the purities of synthesized compounds for biological testing were >95% determined by analytical HPLC. (The purities of **15**, **S4**, and **S6** were 94.9%, 91.9%, and 90.2%, respectively.) Analytical HPLC were carried out using Corona CAD (Charged Aerosol Detector) or photo diode array detector. The column was a Capcell Pak C18AQ (50 mm × 3.0 mm I.D., Shiseido, Japan) or L-column 2 ODS (30 mm × 2.0 mm I.D., CERI, Japan) with a temperature of 50 °C and a flow rate of 0.5 mL/min. Mobile phases A and B under a neutral condition were a mixture of 50 mM AcONH₄, water, and MeCN (1:8:1, v/v/v) and a mixture of 50 mM AcONH₄ and MeCN (1:9, v/v), respectively. The ratio of mobile phase B was increased linearly from 5 to 95% over 3 min, 95% over the next 1 min. Mobile phases A and B under an acidic condition were a mixture of 0.2% formic acid in 10 mM ammonium formate and 0.2% formic acid in MeCN, respectively. The ratio of mobile phase B was increased linearly from 14 to 86% over 3 min, 86% over the next 1 min. Reaction progress was determined by thin layer chromatography

(TLC) analysis on Merck Kieselgel 60 F254 plates or Fuji Silysia NH plates. Chromatographic purification was carried out on silica gel columns (Merck Kieselgel 60, 70–230 mesh or 230–400 mesh, Merck; Chromatorex NH-DM 1020, 100–200 mesh, Fuji Silysia Chemical; Inject column and Universal column, YAMAZEN, <http://yamazenusa.com/products/columns/>; or Purif-Pack Si or NH, Shoko Scientific, <http://shoko-sc.co.jp/english2/>). Preparative HPLC was performed on a Gilson Preparative HPLC System using a YMC-Actus Triart C18 column (150 mm × 20 mm I.D., 5 μm, YMC). Condition 1: Mobile phases A and B under an acidic condition were 0.1% TFA in water and 0.1% TFA in MeCN, respectively. Condition 2: Mobile phases A and B under a neutral condition were 10 mM ammonium bicarbonate and MeCN, respectively. The ratio of mobile phase B was increased linearly in 5-10 min. All commercially available solvents and reagents were used without further purification. Yields were not optimized.

6-(Furan-2-yl)-2-phenethyl-3*H*-imidazo[4,5-*b*]pyridine (1). A mixture of 6-bromo-2-phenethyl-3*H*-imidazo[4,5-*b*]pyridine (**36**) (150 mg, 0.497 mmol), 2-(tributylstannyl)furan (0.18 M DMF solution, 5.0 mL), PdCl₂(PPh₃)₂ (17 mg, 0.024 mmol) was stirred at 80 °C under Ar for 18 h. The mixture was poured into water at room temperature and extracted with EtOAc-THF. The organic layer was separated, washed with water and brine, dried

over MgSO_4 , and concentrated in vacuo. The residue was purified by column chromatography (silica gel, eluted with 50% EtOAc in chloroform) to give **1** (72 mg, 50%) as a white solid. ^1H NMR (300 MHz, $\text{DMSO}-d_6$) δ 3.10-3.20 (4H, m), 6.62 (1H, td, $J = 3.3, 1.8$ Hz), 7.02 (1H, dd, $J = 8.3, 3.3$ Hz), 7.15-7.22 (1H, m), 7.24-7.30 (4H, m), 7.78 (1H, dd, $J = 4.2, 1.2$ Hz), 8.00-8.18 (1H, m), 8.60-8.74 (1H, m), 12.56-13.01 (1H, m). MS m/z : 290.1 $[\text{M} + \text{H}]^+$. HPLC purity 96.0%.

6-(Furan-2-yl)-2-phenyl-3H-imidazo[4,5-*b*]pyridine (2). Compound **2** was prepared from 6-bromo-2-phenyl-3H-imidazo[4,5-*b*]pyridine (**37**) in a manner similar to that described for the synthesis of **1** and obtained (57% yield) as a white solid. ^1H NMR (300 MHz, $\text{DMSO}-d_6$) δ 6.65 (1H, dd, $J = 3.4, 1.9$ Hz), 7.07-7.10 (1H, m), 7.53-7.63 (3H, m), 7.81 (1H, dd, $J = 1.8, 0.7$ Hz), 8.19-8.28 (3H, m), 8.77 (1H, d, $J = 2.0$ Hz). MS m/z : 262.1 $[\text{M} + \text{H}]^+$. HPLC purity 99.2%.

2-Benzyl-6-(furan-2-yl)-3H-imidazo[4,5-*b*]pyridine (3). Compound **3** was prepared from 2-benzyl-6-bromo-3H-imidazo[4,5-*b*]pyridine (**38**) in a manner similar to that described for the synthesis of **1** and obtained (82% yield) as a white solid. ^1H NMR (300 MHz, $\text{DMSO}-d_6$) δ 4.21 (2H, s), 6.62 (1H, dd, $J = 3.4, 1.8$ Hz), 7.01 (1H, dd, $J = 3.4, 0.7$ Hz), 7.22-7.38 (5H, m), 7.78 (1H, dd, $J = 1.8, 0.7$ Hz), 8.11 (1H, brs), 8.68 (1H, d, $J = 1.8$ Hz), 12.70-13.04 (1H, m). MS m/z : 276.1 $[\text{M} + \text{H}]^+$. HPLC purity 99.4%.

2-(2-Chlorophenethyl)-6-(furan-2-yl)-3*H*-imidazo[4,5-*b*]pyridine (4). A mixture of 6-bromo-2-(2-chlorophenethyl)-3*H*-imidazo[4,5-*b*]pyridine (**39**) (200 mg, 0.594 mmol), furan-2-ylboronic acid (100 mg, 0.894 mmol), Pd(PPh₃)₄ (60 mg, 0.052 mmol), 2 M Na₂CO₃ aq. (1.8 mL) in toluene (4 mL), THF (1 mL) and DMF (2 mL) was stirred at 110 °C under Ar for 12 h. The mixture was poured into water at room temperature and extracted with EtOAc. The organic layer was separated, washed with water and brine, dried over MgSO₄, and concentrated in vacuo. The residue was purified by column chromatography (silica gel, eluted with 33% - 100% EtOAc in hexane) to give **4** (90 mg, 47%) as a white solid. ¹H NMR (300 MHz, DMSO-*d*₆) δ 3.13-3.29 (4H, m), 6.62 (1H, dd, *J* = 3.4, 1.8 Hz), 7.02 (1H, dd, *J* = 3.4, 0.7 Hz), 7.22-7.47 (4H, m), 7.78 (1H, dd, *J* = 1.8, 0.7 Hz), 8.12 (1H, d, *J* = 1.9 Hz), 8.68 (1H, d, *J* = 2.0 Hz), 12.74-12.96 (1H, m). MS *m/z*: 324.1 [M + H]⁺. HPLC purity 98.7%.

2-(3-Chlorophenethyl)-6-(furan-2-yl)-3*H*-imidazo[4,5-*b*]pyridine (5). Compound **5** was prepared from 6-bromo-2-(3-chlorophenethyl)-3*H*-imidazo[4,5-*b*]pyridine (**40**) in a manner similar to that described for the synthesis of **4** and obtained (17% yield) as a pale yellow solid. ¹H NMR (300 MHz, DMSO-*d*₆) δ 3.17 (4H, s), 6.62 (1H, dd, *J* = 3.4, 1.8 Hz), 7.02 (1H, dd, *J* = 3.4, 0.7 Hz), 7.21-7.38 (4H, m), 7.78 (1H, dd, *J* = 1.8, 0.7 Hz), 8.11 (1H, d, *J* = 1.7 Hz), 8.67 (1H, d, *J* = 2.0 Hz), 12.59-13.00 (1H, brs). MS *m/z*: 324.2 [M + H]⁺. HPLC purity 97.7%.

2-(4-Chlorophenethyl)-6-(furan-2-yl)-3*H*-imidazo[4,5-*b*]pyridine (6). Compound **6** was prepared from 6-bromo-2-(4-chlorophenethyl)-3*H*-imidazo[4,5-*b*]pyridine (**41**) in a manner similar to that described for the synthesis of **4** and obtained (28% yield) as a pale yellow solid. ¹H NMR (300 MHz, DMSO-*d*₆) δ 3.15 (4H, s), 6.62 (1H, dd, *J* = 3.4, 1.8 Hz), 7.02 (1H, d, *J* = 3.0 Hz), 7.26-7.36 (4H, m), 7.78 (1H, d, *J* = 1.2 Hz), 8.14 (1H, brs), 8.66 (1H, brs), 12.51-13.02 (1H, m). MS *m/z*: 324.1 [M + H]⁺. HPLC purity 98.7%.

6-(Furan-2-yl)-2-(4-methylphenethyl)-3*H*-imidazo[4,5-*b*]pyridine (7). Compound **7** was prepared from 6-bromo-2-(4-methylphenethyl)-3*H*-imidazo[4,5-*b*]pyridine (**42**) in a manner similar to that described for the synthesis of **4** and obtained (63% yield) as a white solid. ¹H NMR (300 MHz, DMSO-*d*₆) δ 2.24 (3H, s), 3.11 (4H, brs), 6.58-6.66 (1H, m), 6.98-7.19 (5H, m), 7.78 (1H, s), 7.99-8.21 (1H, m), 8.59-8.76 (1H, m), 12.50-13.13 (1H, m). MS *m/z*: 304.3 [M + H]⁺. HPLC purity 100.0%.

6-(Furan-2-yl)-2-(4-methoxyphenethyl)-3*H*-imidazo[4,5-*b*]pyridine (8). Compound **8** was prepared from 6-bromo-2-(4-methoxyphenethyl)-3*H*-imidazo[4,5-*b*]pyridine (**43**) in a manner similar to that described for the synthesis of **4** and obtained (28% yield) as a white solid. ¹H NMR (300 MHz, DMSO-*d*₆) δ 3.02-3.16 (4H, m), 3.70 (3H, s), 6.62 (1H, dd, *J* = 3.4, 1.8 Hz), 6.80-6.87 (2H, m), 7.02 (1H, d, *J* = 4.1 Hz), 7.14-7.21 (2H, m), 7.78 (1H, dd, *J* = 1.8, 0.7 Hz),

8.10 (1H, d, $J = 1.8$ Hz), 8.66 (1H, d, $J = 2.0$ Hz), 12.40-13.06 (1H, m). MS m/z : 320.2 $[M + H]^+$.

HPLC purity 99.2%.

2-(4-Fluorophenethyl)-6-(furan-2-yl)-3H-imidazo[4,5-*b*]pyridine (9). Compound **9** was prepared from 6-bromo-2-(4-fluorophenethyl)-3H-imidazo[4,5-*b*]pyridine (**44**) in a manner similar to that described for the synthesis of **4** and obtained (51% yield) as a white solid. ^1H NMR (300 MHz, DMSO- d_6) δ 3.14 (4H, s), 6.62 (1H, dd, $J = 3.3, 1.8$ Hz), 6.99-7.14 (3H, m), 7.25-7.34 (2H, m), 7.78 (1H, s), 7.99-8.20 (1H, m), 8.60-8.75 (1H, m), 12.52-13.01 (1H, m). MS m/z : 308.1 $[M + H]^+$. HPLC purity 96.9%.

6-(Furan-2-yl)-2-(4-(trifluoromethyl)phenethyl)-3H-imidazo[4,5-*b*]pyridine (10). Compound **10** was prepared from 6-bromo-2-(4-(trifluoromethyl)phenethyl)-3H-imidazo[4,5-*b*]pyridine (**45**) in a manner similar to that described for the synthesis of **4** and obtained (48% yield) as a white solid. ^1H NMR (300 MHz, DMSO- d_6) δ 3.19-3.26 (4H, m), 6.62 (1H, dd, $J = 3.4, 1.8$ Hz), 7.02 (1H, dd, $J = 3.4, 0.7$ Hz), 7.50 (2H, d, $J = 7.9$ Hz), 7.65 (2H, d, $J = 8.0$ Hz), 7.78 (1H, dd, $J = 1.8, 0.7$ Hz), 8.11 (1H, d, $J = 2.0$ Hz), 8.67 (1H, d, $J = 2.0$ Hz). MS m/z : 358.3 $[M + H]^+$. HPLC purity 99.0%.

4-(2-(6-(Furan-2-yl)-3H-imidazo[4,5-*b*]pyridin-2-yl)ethyl)benzonitrile (11). Compound **11** was prepared from 4-(2-(6-bromo-3H-imidazo[4,5-*b*]pyridin-2-yl)ethyl)benzonitrile (**46**) in a

manner similar to that described for the synthesis of **4** and obtained (19% yield) as a white solid.

¹H NMR (300 MHz, DMSO-*d*₆) δ 3.16-3.28 (4H, m), 6.62 (1H, dd, *J* = 3.4, 1.8 Hz), 7.02 (1H, dd, *J* = 3.4, 0.7 Hz), 7.46-7.51 (2H, m), 7.72-7.79 (3H, m), 8.11 (1H, d, *J* = 1.9 Hz), 8.67 (1H, d, *J* = 2.0 Hz), 12.82 (1H, brs). MS *m/z*: 315.2 [*M* + *H*]⁺. HPLC purity 99.2%.

2-(4-Fluorophenethyl)-6-phenyl-3*H*-imidazo[4,5-*b*]pyridine (12). Compound **12** was prepared from **44** and phenylboronic acid in a manner similar to that described for the synthesis of **4** and obtained (35% yield) as a white solid. ¹H NMR (300 MHz, DMSO-*d*₆) δ 3.16 (4H, s), 7.06-7.15 (2H, m), 7.26-7.34 (2H, m), 7.35-7.42 (1H, m), 7.46-7.53 (2H, m), 7.69-7.76 (2H, m), 8.11 (1H, d, *J* = 2.1 Hz), 8.56 (1H, d, *J* = 2.1 Hz). MS *m/z*: 318.0 [*M* + *H*]⁺. HPLC purity 98.6%.

2-(4-Fluorophenethyl)-6-(thiophen-2-yl)-3*H*-imidazo[4,5-*b*]pyridine (13). Compound **13** was prepared from **44** in a manner similar to that described for the synthesis of **17** and obtained (29% yield) as a white solid. ¹H NMR (300 MHz, DMSO-*d*₆) δ 3.15 (4H, s), 7.02-7.13 (2H, m), 7.15-7.20 (1H, m), 7.24-7.36 (2H, m), 7.51-7.62 (2H, m), 8.10 (1H, brs), 8.58 (1H, brs), 12.18-13.11 (1H, brs). MS *m/z*: 324.1 [*M* + *H*]⁺. HPLC purity 99.8%.

2-(4-Fluorophenethyl)-6-(3-methylthiophen-2-yl)-3*H*-imidazo[4,5-*b*]pyridine (14).

Compound **14** was prepared from **44** and (3-methylthiophen-2-yl)boronic acid in a manner similar to that described for the synthesis of **17** and obtained (19% yield) as a white solid. ¹H

NMR (300 MHz, DMSO- d_6) δ 2.28 (3H, s), 3.15 (4H, s), 7.02-7.14 (3H, m), 7.26-7.34 (2H, m), 7.50 (1H, d, J = 5.1 Hz), 7.91 (1H, d, J = 2.1 Hz), 8.33 (1H, d, J = 2.1 Hz). MS m/z : 338.1 [$M + H$] $^+$. HPLC purity 100.0%.

2-(4-Fluorophenethyl)-6-(4-methylthiophen-2-yl)-3*H*-imidazo[4,5-*b*]pyridine (15).

Compound **15** was prepared from **44** and (4-methylthiophen-2-yl)boronic acid in a manner similar to that described for the synthesis of **17** and obtained (10% yield) as a pale yellow solid.

^1H NMR (300 MHz, DMSO- d_6) δ 2.25 (3H, d, J = 0.8 Hz), 3.14 (4H, s), 7.05-7.14 (3H, m), 7.25-7.33 (2H, m), 7.38 (1H, d, J = 1.2 Hz), 8.03 (1H, d, J = 2.1 Hz), 8.53 (1H, d, J = 2.1 Hz), 12.66-12.90 (1H, brs). MS m/z : 338.1 [$M + H$] $^+$. HPLC purity 94.9%.

2-(4-Fluorophenethyl)-6-(5-methylthiophen-2-yl)-3*H*-imidazo[4,5-*b*]pyridine (16).

Compound **16** was prepared from **44** and (5-methylthiophen-2-yl)boronic acid in a manner similar to that described for the synthesis of **17** and obtained (29% yield) as a pale yellow solid.

^1H NMR (300 MHz, CD $_3$ OD) δ 2.53 (3H, d, J = 0.9 Hz), 3.14-3.27 (4H, m), 6.77-6.84 (1H, m), 6.94-7.03 (2H, m), 7.19-7.28 (3H, m), 8.01 (1H, brs), 8.55 (1H, s). MS m/z : 338.1 [$M + H$] $^+$. HPLC purity 97.5%.

2-((4-Fluorophenoxy)methyl)-6-(thiophen-2-yl)-3*H*-imidazo[4,5-*b*]pyridine (17). A mixture of **29** (50 mg, 0.16 mmol), thiophen-2-ylboronic acid (26 mg, 0.20 mmol), Pd(Amphos)Cl $_2$ (11

mg, 0.016 mmol), Na₂CO₃ (82 mg, 0.78 mmol), DME (1.25 mL) and water (0.25 mL) was heated at 120 °C for 2 h under microwave irradiation. The mixture was poured into water at room temperature and extracted with EtOAc. The organic layer was separated, dried over MgSO₄, and concentrated in vacuo. The residue was purified by column chromatography (NH silica gel, eluted with 50% - 80% EtOAc in hexane) to give the crude product as a white solid. This solid was dissolved in DMSO and purified by preparative HPLC under a neutral condition to give **17** (8.7 mg, 17%) as a white solid. ¹H NMR (300 MHz, DMSO-*d*₆) δ 5.34 (2H, s), 7.09-7.20 (5H, m), 7.56-7.61 (2H, m), 8.16 (1H, d, *J* = 2.1 Hz), 8.67 (1H, d, *J* = 2.1 Hz). MS *m/z*: 326.1 [M + H]⁺. HPLC purity 99.2%.

2-(Phenoxymethyl)-6-(thiophen-2-yl)-3*H*-imidazo[4,5-*b*]pyridine (18). Compound **18** was prepared from 6-bromo-2-(phenoxymethyl)-3*H*-imidazo[4,5-*b*]pyridine (**47**) in a manner similar to that described for the synthesis of **17** and obtained (42% yield) as a brown solid. ¹H NMR (300 MHz, DMSO-*d*₆) δ 5.31-5.40 (2H, m), 6.95-7.02 (1H, m), 7.07-7.13 (2H, m), 7.18 (1H, dd, *J* = 5.1, 3.7 Hz), 7.28-7.37 (2H, m), 7.59 (2H, td, *J* = 4.0, 1.2 Hz), 8.17 (1H, brs), 8.68 (1H, d, *J* = 2.1 Hz), 13.23 (1H, brs). MS *m/z*: 308.2 [M + H]⁺. HPLC purity 98.6%.

6-(3-Isopropylthiophen-2-yl)-2-(phenoxymethyl)-3*H*-imidazo[4,5-*b*]pyridine (19). To a solution of **47** (500 mg, 1.65 mmol), bis(pinacolato)diboron (1.25 g, 4.95 mmol) and potassium

acetate (970 mg, 9.90 mmol) in DMF (15 mL) was added PdCl₂(dppf) (134 mg, 0.183 mmol) at room temperature. The mixture was heated at 110 °C for 1 h under microwave irradiation. The mixture was filtered through a celite bed and washed with EtOAc. The filtrate was poured into water. The organic layer was separated, dried over Na₂SO₄, and concentrated in vacuo to give 2-(phenoxyethyl)-6-(4,4,5,5-tetramethyl-1,3,2-dioxaborolan-2-yl)-3*H*-imidazo[4,5-*b*]pyridine (800 mg, crude) as a black semi-solid. This product was subjected to the next reaction without further purification. MS *m/z*: 270.21 [M + H]⁺.

To a solution of the crude product (798 mg, 2.27 mmol) and Na₂CO₃ (547 mg, 5.17 mmol) in 1,4-dioxane (6 mL) and water (2 mL) were added 2-bromo-3-isopropylthiophene (212 mg, 1.03 mmol), Pd(Amphos)Cl₂ (73 mg, 0.10 mmol) at room temperature. The mixture was heated at 100 °C for 2 h under microwave irradiation. The mixture was filtered through a celite bed and washed with EtOAc. The organic layer was separated, washed with water and brine, dried over Na₂SO₄, and concentrated in vacuo to give the crude product. The crude product was purified by column chromatography (silica gel, eluted with 30% EtOAc in petroleum ether), followed by preparative HPLC under a neutral condition to give **19** (16 mg, 3%, overall yield on 2-steps) as an off white solid. ¹H NMR (500 MHz, DMSO-*d*₆) δ 1.19 (6H, d, *J* = 6.71 Hz), 3.02-3.05 (1H, m), 5.35 (2H, s), 6.99 (1H, t, *J* = 7.3 Hz), 7.10 (2H, d, *J* = 7.9 Hz), 7.20 (1H, d, *J* = 5.2 Hz), 7.30-7.33 (2H, m),

7.53 (1H, d, $J = 5.5$ Hz), 7.89 (1H, d, $J = 2.1$ Hz), 8.30 (1H, d, $J = 1.8$ Hz), 13.34 (1H, brs). MS m/z : 350.31 $[M + H]^+$. HPLC purity 95.7%.

2-(4-Fluorophenethyl)-6-(thiophen-2-yl)oxazolo[5,4-*b*]pyridine (20). To a solution of 3-amino-5-bromopyridin-2-ol (500 mg, 2.65 mmol) in toluene (10 mL) and acetic acid (10 mL) was added **32** (3.02 g, 13.3 mmol) and the mixture was refluxed for 12 h. After cooling to room temperature, the mixture was concentrated under reduced pressure and the residue was purified by column chromatography (silica gel, eluted with 0% - 10% EtOAc in hexane) to give 6-bromo-2-(4-fluorophenethyl)oxazolo[5,4-*b*]pyridine (115 mg, 14%) as an off white solid. ^1H NMR (400 MHz, CDCl_3) δ 3.10-3.30 (4H, m), 6.97 (2H, t, $J = 8.6$ Hz), 7.16-7.21 (2H, m), 8.08 (1H, d, $J = 2.1$ Hz), 8.36 (1H, d, $J = 2.1$ Hz). MS m/z : 320.94 $[M + H]^+$.

A mixture of 6-bromo-2-(4-fluorophenethyl)oxazolo[5,4-*b*]pyridine (61 mg, 0.19 mmol), thiophen-2-ylboronic acid (37 mg, 0.29 mmol) and Na_2CO_3 (50 mg, 0.48 mmol) in 1,4-dioxane (5 mL) and water (1 mL) was degassed with argon for 10 min. To the resulting mixture was added $\text{PdCl}_2(\text{PPh}_3)_2$ (14 mg, 0.019 mmol) and heated at 110 °C for 1 h. The mixture was filtered through a celite bed and the filtrate was concentrated under reduced pressure. The residue was purified by column chromatography (silica gel, eluted with 0% - 15% EtOAc in hexane) to give **20** (45 mg, 74%) as a yellow solid. ^1H NMR (400 MHz, $\text{DMSO}-d_6$) δ 3.16 (2H, t, $J = 7.6$ Hz),

3.28-3.33 (2H, m), 7.11 (2H, t, $J = 8.9$ Hz), 7.18-7.21 (1H, m), 7.30-7.36 (2H, m), 7.62-7.67 (2H, m), 8.42 (1H, d, $J = 2.1$ Hz), 8.62 (1H, d, $J = 2.0$ Hz). MS m/z : 325.3 $[M + H]^+$. HPLC purity 96.0%.

2-(4-Fluorophenethyl)-6-(thiophen-2-yl)oxazolo[4,5-*b*]pyridine (21). To a solution of **33** (121 mg, 0.629 mmol) in toluene (2 mL) and AcOH (2 mL) was added **32** (428 mg, 1.87 mmol) and the mixture was refluxed for 5 h. After cooling to room temperature, the mixture was concentrated under reduced pressure and the residue was purified by column chromatography (silica gel, eluted with 0% - 30% EtOAc in hexane) to give **21** (150 mg, 73%) as an off white solid. ^1H NMR (400 MHz, DMSO- d_6) δ 3.17 (2H, t, $J = 7.6$ Hz), 3.28-3.37 (2H, m), 7.11 (2H, t, $J = 8.8$ Hz), 7.18-7.23 (1H, m), 7.31-7.37 (2H, m), 7.65-7.70 (2H, m), 8.44 (1H, d, $J = 1.9$ Hz), 8.79 (1H, d, $J = 1.9$ Hz). MS m/z : 325.2 $[M + H]^+$. HPLC purity 98.9%.

2-(4-Fluorophenethyl)-5-(thiophen-2-yl)-1*H*-benzo[*d*]imidazole (22). Compound **22** was prepared from 5-bromo-2-(4-fluorophenethyl)-1*H*-benzo[*d*]imidazole (**48**) in a manner similar to that described for the synthesis of **17** and obtained (50% yield) as a white solid. ^1H NMR (300 MHz, DMSO- d_6) δ 3.11 (4H, s), 7.05-7.15 (3H, m), 7.25-7.33 (2H, m), 7.39-7.52 (4H, m), 7.71 (1H, brs), 12.32 (1H, brs). MS m/z : 323.1 $[M + H]^+$. HPLC purity 97.3%.

2-(4-Fluorophenethyl)-5-methyl-6-(thiophen-2-yl)-3*H*-imidazo[4,5-*b*]pyridine (23). A solution of 6-bromo-2-(4-fluorophenethyl)-5-methyl-3*H*-imidazo[4,5-*b*]pyridine (**49**) (150 mg, 0.449 mmol) and thiophen-2-ylboronic acid (86 mg, 0.67 mmol) in 1,4-dioxane (8 mL) and water (2 mL) was degassed with argon for 10 min. To the mixture were added PdCl₂(PPh₃)₂ (31.5 mg, 0.0449 mmol) and Na₂CO₃ (119 mg, 1.12 mmol). The resulting mixture was heated at 110°C for 16 h. After cooling to room temperature, the mixture was filtered through a celite bed. The filtrate was concentrated in vacuo and the residue was purified by column chromatography (silica gel, eluted with 15% - 20% EtOAc in hexane) to give **23** (40 mg, 26%) as a white solid. ¹H NMR (400 MHz, DMSO-*d*₆) δ 2.58 (3H, s), 3.14 (4H, s), 7.05 (2H, t, *J* = 8.7 Hz), 7.10-7.20 (2H, m), 7.25-7.40 (2H, m), 7.56 (1H, s), 7.79 (1H, s), 12.41 (1H, brs). MS *m/z*: 338.0 [M + H]⁺. HPLC purity 99.3%.

2-(4-Fluorophenethyl)-7-methyl-6-(thiophen-2-yl)-3*H*-imidazo[4,5-*b*]pyridine (24).

Compound **24** was prepared from 6-bromo-2-(4-fluorophenethyl)-7-methyl-3*H*-imidazo[4,5-*b*]pyridine (**50**) in a manner similar to that described for the synthesis of **17** and obtained (34% yield) as a white solid. ¹H NMR (300 MHz, DMSO-*d*₆) δ 2.58 (3H, s), 3.14 (4H, s), 7.06-7.15 (2H, m), 7.17-7.24 (2H, m), 7.27-7.35

(2H, m), 7.65 (1H, dd, $J = 5.1, 1.3$ Hz), 8.25 (1H, s), 12.66-12.92 (1H, m). MS m/z : 338.1 $[M + H]^+$. HPLC purity 99.4%.

***N*-Methyl-2-(2-(phoxymethyl)-3*H*-imidazo[4,5-*b*]pyridin-6-yl)thiophene-3-carboxamide**

(**25**). To a solution of **47** (1.8 g, 5.9 mmol) in dichloromethane (20 mL) was added DIPEA (2.1 mL, 12 mmol) and 2-(chloromethoxy)ethyltrimethylsilane (1.3 mL, 7.1 mmol) at 0 °C. The mixture was stirred at 25 °C for 12 h. The mixture was diluted with dichloromethane and washed with water and brine. The organic layer was separated, dried over Na_2SO_4 , and concentrated in vacuo to give 6-bromo-2-(phoxymethyl)-3-((2-(trimethylsilyl)ethoxy)methyl)-3*H*-imidazo[4,5-*b*]pyridine (1.7 g, 66%) as a yellow oil. MS m/z : 434.1 $[M + H]^+$.

A mixture of 6-bromo-2-(phoxymethyl)-3-((2-(trimethylsilyl)ethoxy)methyl)-3*H*-imidazo[4,5-*b*]pyridine (1.5 g, 3.5 mmol), bis(pinacolato)diboron (1.1 g, 4.1 mmol), potassium acetate (1.0 g, 10 mmol) and $PdCl_2(dppf)$ (253 mg, 0.345 mmol) in 1,4-dioxane (15 mL) was stirred at 90 °C under N_2 for 8 h. The mixture was concentrated in vacuo. The residue was purified by column chromatography (silica gel, eluted with 5% - 20% EtOAc in petroleum ether) to give

2-(phenoxyethyl)-6-(4,4,5,5-tetramethyl-1,3,2-dioxaborolan-2-yl)-3-((2-(trimethylsilyl)ethoxy)methyl)-3*H*-imidazo[4,5-*b*]pyridine (1.5 g, 90%) as a yellow solid. MS *m/z*: 482.1 [*M* + *H*]⁺.

To a solution of

2-(phenoxyethyl)-6-(4,4,5,5-tetramethyl-1,3,2-dioxaborolan-2-yl)-3-((2-(trimethylsilyl)ethoxy)methyl)-3*H*-imidazo[4,5-*b*]pyridine

(100 mg, 0.208 mmol) and

2-bromo-*N*-methyl-thiophene-3-carboxamide (46 mg, 0.21 mmol) in water (1 mL) and

1,4-dioxane (5 mL) were added potassium carbonate (72 mg, 0.52 mmol) and PdCl₂(dppf) (15

mg, 0.021 mmol) at room temperature. The mixture was stirred at 90 °C under N₂ for 8 h. The

mixture was poured into water at room temperature and extracted with EtOAc. The organic

layer was separated, washed with brine, dried over Na₂SO₄, and concentrated in vacuo. The

residue was purified by column chromatography (silica gel, 5% - 30% EtOAc in petroleum ether)

to give

N-methyl-2-(2-(phenoxyethyl)-3-((2-(trimethylsilyl)ethoxy)methyl)-3*H*-imidazo[4,5-*b*]pyridin-

6-yl)thiophene-3-carboxamide (75 mg, 73% yield) as a yellow solid. MS *m/z*: 495.1 [*M* + *H*]⁺.

A mixture of

N-methyl-2-(2-(phenoxyethyl)-3-((2-(trimethylsilyl)ethoxy)methyl)-3*H*-imidazo[4,5-*b*]pyridin-

6-yl)thiophene-3-carboxamide (70 mg, 0.14 mmol) in dichloromethane (3 mL) and TFA (1 mL)

was stirred at 25 °C for 12 h. The mixture was concentrated in vacuo. The residue was purified by preparative HPLC under an acidic condition to give **25** (26 mg, 50%) as a white solid. ¹H NMR (400 MHz, DMSO-*d*₆) δ 2.65 (3H, d, *J* = 4.8 Hz), 5.40 (2H, s), 6.99 (1H, t, *J* = 7.2 Hz), 7.10 (2H, d, *J* = 8.0 Hz), 7.31-7.36 (3H, m), 7.65 (1H, d, *J* = 5.2 Hz), 8.03-8.07 (1H, m), 8.11 (1H, d, *J* = 4.8 Hz), 8.43 (1H, d, *J* = 2.0 Hz). MS *m/z*: 365.1 [M + H]⁺. HPLC purity 98.6%.

***N*-Methyl-5-(2-(phenoxymethyl)-3*H*-imidazo[4,5-*b*]pyridin-6-yl)thiophene-3-carboxamide**

(26). Compound **26** was prepared from methanamine in a manner similar to that described for the synthesis of **28** and obtained (57% yield) as a white solid. ¹H NMR (300 MHz, DMSO-*d*₆) δ 2.78 (3H, d, *J* = 4.5 Hz), 5.36 (2H, s), 6.95-7.02 (1H, m), 7.08-7.13 (2H, m), 7.29-7.36 (2H, m), 7.89 (1H, d, *J* = 1.4 Hz), 8.07 (1H, d, *J* = 1.4 Hz), 8.15 (1H, d, *J* = 2.1 Hz), 8.30 (1H, d, *J* = 4.4 Hz), 8.65 (1H, d, *J* = 2.2 Hz). MS *m/z*: 365.2 [M + H]⁺. HPLC purity 98.8%.

***N*-(2-(2-Methoxyethoxy)ethyl)-5-(2-(phenoxymethyl)-3*H*-imidazo[4,5-*b*]pyridin-6-yl)thiophene-3-carboxamide (27).**

Compound **27** was prepared from 2-(2-methoxyethoxy)ethan-1-amine in a manner similar to that described for the synthesis of **28** and obtained (56% yield) as a white solid. ¹H NMR (300 MHz, DMSO-*d*₆) δ 3.24 (3H, s), 3.37-3.48 (4H, m), 3.51-3.58 (4H, m), 5.36 (2H, s), 6.95-7.02 (1H, m), 7.07-7.14 (2H, m), 7.29-7.37 (2H, m), 7.93 (1H, d, *J* = 1.4 Hz), 8.12

(1H, d, $J = 1.4$ Hz), 8.16 (1H, d, $J = 2.1$ Hz), 8.40 (1H, t, $J = 5.6$ Hz), 8.65 (1H, d, $J = 2.2$ Hz), 12.98-13.53 (1H, m). MS m/z : 453.3 $[M + H]^+$. HPLC purity 95.2%.

***N*-(2-(3-(But-3-yn-1-yl)-3*H*-diazirin-3-yl)ethyl)-5-(2-(phoxymethyl)-3*H*-imidazo[4,5-*b*]pyr**

idin-6-yl)thiophene-3-carboxamide (28). A mixture of

2-(3-(but-3-yn-1-yl)-3*H*-diazirin-3-yl)ethan-1-amine (12 mg, 0.087 mmol), **35** (30 mg, 0.085 mmol), HATU (39 mg, 0.10 mmol) and DIPEA (18 μ L, 0.10 mmol) in DMF (0.6 mL) was stirred at room temperature for 1 h. The mixture was purified by column chromatography (NH silica gel, eluted with 0% - 15% MeOH in EtOAc) to give **28** (26 mg, 65%) as a white solid. ^1H NMR (300 MHz, DMSO- d_6) δ 1.65 (4H, q, $J = 7.3$ Hz), 1.98-2.06 (2H, m), 2.85 (1H, t, $J = 2.6$ Hz), 3.05-3.26 (2H, m), 5.38 (2H, s), 6.96-7.03 (1H, m), 7.08-7.14 (2H, m), 7.29-7.37 (2H, m), 7.91 (1H, d, $J = 1.3$ Hz), 8.08-8.25 (2H, m), 8.36 (1H, t, $J = 5.6$ Hz), 8.68 (1H, d, $J = 2.1$ Hz), 12.98-13.62 (1H, m). MS m/z : 471.2 $[M + H]^+$. HPLC purity 99.2%.

6-Bromo-2-((4-fluorophenoxy)methyl)-3*H*-imidazo[4,5-*b*]pyridine (29). To a solution of 5-bromopyridine-2,3-diamine (1.50 g, 7.98 mmol), HATU (3.34 g, 8.78 mmol) and DIPEA (1.53 mL, 8.78 mmol) in DMF (8 mL) was added 2-(4-fluorophenoxy)acetic acid (1.36 g, 7.98 mmol) at room temperature. The mixture was stirred at room temperature for 1 h. The mixture was poured into water at room temperature and extracted with EtOAc. The organic layer was

separated, washed with water and brine, dried over MgSO_4 , and concentrated in vacuo. To the residue was added AcOH (10 mL) and the mixture was refluxed overnight. The mixture was quenched with sat. NaHCO_3 aq. at room temperature. The precipitate was collected by filtration and washed with water and EtOAc to give **29** (1.8 g, 70%) as a pale purple solid. MS m/z: 322.0 $[\text{M} + \text{H}]^+$.

3-(4-Fluorophenyl)propanamide (30). To a stirred solution of 3-(4-fluorophenyl)propanoic acid (5.0 g, 30 mmol) in chloroform (20 mL) was added DMF (0.231 mL, 2.97 mmol) and oxalyl chloride (2.80 mL, 32.7 mmol) at room temperature. The mixture was stirred at room temperature for 2 h and concentrated in vacuo. The residue was dissolved in chloroform (50 mL), and NH_3 gas was passed through the solution at 0 °C for 30 min. The mixture was stirred at room temperature for 2 h and diluted with dichloromethane and water. The organic layer was separated, washed with brine, dried over Na_2SO_4 , and concentrated under reduced pressure. The residue was purified by column chromatography (silica gel, eluted with 50% - 70% EtOAc in hexane) to give **30** (3.8 g, 76%) as white solid. ^1H NMR (400 MHz, CDCl_3) δ 2.49 (2H, t, $J = 7.7$ Hz), 2.91-2.95 (2H, m), 5.30-5.55 (2H, m), 6.96 (2H, t, $J = 8.6$ Hz), 7.13-7.19 (2H, m). MS m/z: 168.0 $[\text{M} + \text{H}]^+$.

3-(4-Fluorophenyl)propanenitrile (31). Compound **30** (2.5 g, 15 mmol) was dissolved in trifluoroacetic anhydride (8 mL) and the resulting mixture was stirred at room temperature overnight. The mixture was concentrated under reduced pressure and the residue was diluted with dichloromethane and 2N NaOH aq. The organic layer was separated, washed with water and brine, dried over Na₂SO₄, and concentrated under reduced pressure. The residue was purified by column chromatography (silica gel, eluted with 0% - 20% EtOAc in hexane) to give **31** (2.0 g, 90%) as a colorless oil. ¹H NMR (400 MHz, CDCl₃) δ 2.60 (2H, t, *J* = 7.3 Hz), 2.93 (2H, t, *J* = 7.3 Hz), 7.02 (2H, t, *J* = 8.6 Hz), 7.17-7.23 (2H, m).

1-Fluoro-4-(3,3,3-trimethoxypropyl)benzene (32). To a solution of **31** (6.5 g, 44 mmol) in anhydrous MeOH (2.12 mL) and anhydrous Et₂O (30 mL) was bubbled HCl gas (freshly generated by adding conc. HCl to conc. H₂SO₄) at 0 °C for 1 h. The mixture was kept at 4 °C under Ar for 24 h. The mixture was concentrated, and to the residue were added anhydrous MeOH (5.30 mL) and hexane (70 mL). The resulting mixture was stirred at room temperature for 48 h and precipitated ammonium chloride was removed by filtration. The filtrate was concentrated under reduced pressure to give a mixture of **32** and the corresponding methyl ester (7.0 g, crude mixture) as a colorless liquid. The mixture was used in the next step without further purification. ¹H NMR (400 MHz, CDCl₃) δ 1.96-2.05 (2H, m), 2.50-2.65 (2H, m), 3.25 (9H, s),

6.95 (2H, t, $J = 8.6$ Hz), 7.10-7.16 (2H, m). [Additional peaks of corresponding ester are also present and some peaks are merged with desired compound. Integration in ^1H NMR showed ca. 57% desired compound.]

2-Amino-5-(thiophen-2-yl)pyridin-3-ol (33). A mixture of 2-amino-5-bromopyridin-3-ol (200 mg, 1.06 mmol), thiophen-2-ylboronic acid (203 mg, 1.59 mmol), $\text{PdCl}_2(\text{PPh}_3)_2$ (74 mg, 0.10 mmol) and Na_2CO_3 (561 mg, 5.29 mmol) in 1,4-dioxane (5 mL) and water (1 mL) was stirred at 110 °C under Ar overnight. After cooling to room temperature, the mixture was filtered through a celite bed. The filtrate was concentrated under reduced pressure and the residue was purified by column chromatography (silica gel, eluted with 0% - 5% MeOH in dichloromethane) to give **33** (120 mg, 59%) as a brown solid. ^1H NMR (400 MHz, $\text{DMSO}-d_6$) δ 5.71 (2H, brs), 7.04-7.08 (2H, m), 7.20-7.25 (1H, m), 7.35-7.42 (1H, m), 7.76 (1H, d, $J = 1.8$ Hz), 9.73 (1H, s). MS m/z : 191.0 $[\text{M} - \text{H}]^-$.

Methyl 5-(2-(phenoxymethyl)-3H-imidazo[4,5-*b*]pyridin-6-yl)thiophene-3-carboxylate (34).

Compound **34** was prepared from **47** and methyl 5-(4,4,5,5-tetramethyl-1,3,2-dioxaborolan-2-yl)thiophene-3-carboxylate in a manner similar to that described for the synthesis of **17** and obtained (42% yield) as a brown solid. MS m/z : 366.1 $[\text{M} + \text{H}]^+$.

5-(2-(Phenoxymethyl)-3*H*-imidazo[4,5-*b*]pyridin-6-yl)thiophene-3-carboxylic acid (35). To a solution of **34** (700 mg, 1.92 mmol) in THF (20 mL) and MeOH (10 mL) was added 2N NaOH aq. (3 mL) at 60 °C. The mixture was stirred at 60 °C for 1 h. The mixture was neutralized with 2N HCl aq. at room temperature and diluted with water. The resulting solid was collected by filtration and washed with water to give **35** (580 mg, 86 %) as a pale yellow solid. MS m/z: 352.1 [M + H]⁺.

6-Bromo-2-phenethyl-3*H*-imidazo[4,5-*b*]pyridine (36). A mixture of 5-bromopyridine-2,3-diamine (1.09 g, 5.80 mmol) and 3-phenylpropanoyl chloride (0.98 g, 5.8 mmol) in diphenylether (0.5 mL) was stirred at 170 °C for 1.5 h. The mixture was diluted with a mixture of chloroform and methanol (10:1) and neutralized with 1N NaOH aq. at room temperature. The organic layer was separated, washed with water and brine, dried over MgSO₄, and concentrated in vacuo. The residue was washed with diethyl ether to give **36** (1.33 g, 76%) as a white solid. MS m/z: 302.1 [M + H]⁺.

6-Bromo-2-phenyl-3*H*-imidazo[4,5-*b*]pyridine (37). A mixture of P₂O₅ (1.70 g, 12.0 mmol) and methanesulfonic acid (6 mL) was stirred at 100 °C for 1 h. To the mixture were added 5-bromopyridine-2,3-diamine (1.13 g, 6.00 mmol) and benzoic acid (0.73 g, 6.0 mmol). The mixture was stirred at 100 °C for 1 h. After cooling to room temperature, the mixture was poured

into 4N NaOH aq. (100 mL) at 0 °C and stirred at room temperature for 40 min. The mixture was neutralized with conc. HCl. The resulting solid was collected by filtration and washed with water and diethyl ether to give **37** (0.79 g, 48%) as a white solid. MS m/z: 273.8 [M + H]⁺.

2-Benzyl-6-bromo-3H-imidazo[4,5-*b*]pyridine (38). Compound **38** was prepared from 2-phenylacetyl chloride in a manner similar to that described for the synthesis of **36** and obtained (71% yield) as a white solid. MS m/z: 288.1 [M + H]⁺.

6-Bromo-2-(2-chlorophenethyl)-3H-imidazo[4,5-*b*]pyridine (39). A mixture of 3-(2-chlorophenyl)propanoic acid (2.42 g, 13.1 mmol), 5-bromopyridine-2,3-diamine (2.44 g, 13.0 mmol), POCl₃ (60 mL) was stirred at 140 °C for 4 h. After cooling to room temperature, the mixture was concentrated in vacuo. The residue was poured into water, neutralized with 1N NaOH aq. and extracted with EtOAc. The organic layer was separated, washed with water and brine, dried over MgSO₄, and concentrated in vacuo. The residue was washed with diisopropyl ether to give **39** (1.95 g, 45%) as a brown solid. MS m/z: 336.0 [M + H]⁺.

6-Bromo-2-(3-chlorophenethyl)-3H-imidazo[4,5-*b*]pyridine (40). Compound **40** was prepared from 3-(3-chlorophenyl)propanoic acid in a manner similar to that described for the synthesis of **39** and obtained (72% yield) as a brown solid. MS m/z: 336.0 [M + H]⁺.

6-Bromo-2-(4-chlorophenethyl)-3*H*-imidazo[4,5-*b*]pyridine (41). Compound **41** was prepared from 3-(4-chlorophenyl)propanoic acid in a manner similar to that described for the synthesis of **39** and obtained (20% yield) as a white solid. MS *m/z*: 336.0 [M + H]⁺.

6-Bromo-2-(4-methylphenethyl)-3*H*-imidazo[4,5-*b*]pyridine (42). Compound **42** was prepared from 3-(*p*-tolyl)propanoic acid in a manner similar to that described for the synthesis of **39** and obtained (35% yield) as a pale yellow solid. MS *m/z*: 316.0 [M + H]⁺.

6-Bromo-2-(4-methoxyphenethyl)-3*H*-imidazo[4,5-*b*]pyridine (43). To a mixture of 3-(4-methoxyphenyl)propanoic acid (1.8 g, 10 mmol) in THF (30 mL) were added oxalyl chloride (1.1 mL, 12 mmol) and DMF (20 μL) at 4 °C. The mixture was stirred at room temperature for 1.5 h. The mixture was concentrated in vacuo and to the residue was added toluene. The solution was concentrated again to remove an excess amount of oxalyl chloride. To the residual oil was added 5-bromopyridine-2,3-diamine (1.7 g, 9.0 mmol) and stirred at 170 °C for 30 min. The mixture was suspended in MeOH and H₂SO₄ at room temperature and stirred at 80 °C for 3 h. After cooling to room temperature, the mixture was concentrated in vacuo. The residue was poured into water, neutralized with sat. NaHCO₃ aq. and extracted with EtOAc. The organic layer was separated, washed with water and brine, dried over MgSO₄, and concentrated

in vacuo. The residue was purified by column chromatography (silica gel, 50% - 80% EtOAc in hexane) to give **43** (600 mg, 20%) as a white solid. MS m/z: 332.1 [M + H]⁺.

6-Bromo-2-(4-fluorophenethyl)-3H-imidazo[4,5-*b*]pyridine (44). Compound **44** was prepared from 3-(4-fluorophenyl)propanoic acid in a manner similar to that described for the synthesis of **29** and obtained (65% yield) as a brown solid. ¹H NMR (300 MHz, DMSO-*d*₆) δ 3.04-3.19 (4H, m), 7.00-7.15 (2H, m), 7.23-7.34 (2H, m), 8.16 (1H, d, *J* = 2.2 Hz), 8.33 (1H, d, *J* = 2.2 Hz), 12.39-13.29 (1H, m). MS m/z: 320.9 [M + H]⁺.

6-Bromo-2-(4-(trifluoromethyl)phenethyl)-3H-imidazo[4,5-*b*]pyridine (45). Compound **45** was prepared from 3-(4-(trifluoromethyl)phenyl)propanoic acid in a manner similar to that described for the synthesis of **39** and obtained (78% yield) as a brown solid. MS m/z: 370.0 [M + H]⁺.

4-(2-(6-Bromo-3H-imidazo[4,5-*b*]pyridin-2-yl)ethyl)benzonitrile (46). Compound **46** was prepared from 3-(4-cyanophenyl)propanoic acid in a manner similar to that described for the synthesis of **39** obtained (79% yield) as a pale yellow solid. MS m/z: 327.0 [M + H]⁺.

6-Bromo-2-(phenoxymethyl)-3H-imidazo[4,5-*b*]pyridine (47). Compound **47** was prepared from 2-phenoxyacetic acid in a manner similar to that described for the synthesis of **29** obtained

(65% yield) as a brown solid. ^1H NMR (300 MHz, $\text{DMSO}-d_6$) δ 5.28-5.43 (2H, m), 6.94-7.03 (1H, m), 7.06-7.15 (2H, m), 7.26-7.39 (2H, m), 8.18-8.31 (1H, m), 8.37-8.50 (1H, m). MS m/z : 304.0 $[\text{M} + \text{H}]^+$.

5-Bromo-2-(4-fluorophenethyl)-1*H*-benzo[*d*]imidazole (48). Compound **48** was prepared from 3-(4-fluorophenyl)propanoic acid and 4-bromobenzene-1,2-diamine in a manner similar to that described for the synthesis of **29** and obtained (60% yield) as a pale yellow solid. MS m/z : 319.0 $[\text{M} + \text{H}]^+$.

6-Bromo-2-(4-fluorophenethyl)-5-methyl-3*H*-imidazo[4,5-*b*]pyridine (49). Compound **49** was prepared from 3-(4-fluorophenyl)propanoic acid and 4-bromo-5-methylbenzene-1,2-diamine in a manner similar to that described for the synthesis of **29** and obtained (88% yield) as a pale yellow solid. ^1H NMR (400 MHz, $\text{DMSO}-d_6$) δ 2.61 (3H, s), 3.00-3.20 (4H, m), 7.08 (2H, t, $J = 8.7$ Hz), 7.26 (2H, t, $J = 5.8$ Hz), 8.13 (1H, s), 12.87 (1H, brs).

6-Bromo-2-(4-fluorophenethyl)-7-methyl-3*H*-imidazo[4,5-*b*]pyridine (50). Compound **50** was prepared from 3-(4-fluorophenyl)propanoic acid and 4-bromo-3-methylbenzene-1,2-diamine in a manner similar to that described for the synthesis of **29** and obtained (36% yield) as a brown solid. MS m/z : 335.1 $[\text{M} + \text{H}]^+$.

Dysferlin Elevation Assay.

Cells and Reagents. Patient-derived iPSCs were established from dermal fibroblasts as previously described.²³ The original dysferlinopathy patient has a compound hetero mutation with both c.2997 G>T (p. W999C) as missense mutation and c.1958 delG as nonsense mutation in dysferlin gene. Cells from a healthy sibling donor were also used as the normal control. Tet-MyoD1 vector was introduced into iPSCs according to previous methods¹⁴ and stably transfected clones were selected for further analysis. These cells were maintained as a feeder-free culture on iMatrix-511 (Nippi. Inc.) in StemFit AK02N (Ajinomoto Healthy Supply Co., Inc.).²⁴ Test compounds were dissolved in DMSO and added to culture medium at the final DMSO concentration of 0.1%. Antibodies used in immunostaining were as follows. Primary antibodies: rabbit anti-dysferlin monoclonal antibody (clone#JAI-1-49-3, Abcam plc.) and mouse anti-myosin heavy chain (MHC) monoclonal antibody (clone#MF20, R&D Systems). Secondary antibodies: Alexa Fluor 488 conjugated goat anti-rabbit IgG and Alexa Fluor 647 conjugated goat anti-mouse IgG (Thermo Fisher Scientific).

Differentiation into myocyte by MyoD induction. The iPSCs were differentiated into myocyte by the inducible expression of MyoD1 as previously described.^{14,25} Briefly, cells were seeded on

matrigel (Corning Inc.) -coated CellCarrier-384 Ultra microplates (PerkinElmer Japan Co., Ltd.) with StemFit AK02N medium containing 10 μ M ROCK inhibitor, Y-27632 (FUJIFILM Wako Pure Chemical Corporation) on "day 0". After 24 h, the medium was changed to Primate ES Cell Medium (REPROCELL Inc.) without basic fibroblast growth factor. After additional 24 h, 1 μ g/mL doxycycline (LKT Laboratories, Inc.) was added to the medium. On day 3, the medium was changed to alpha MEM (Nacalai Tesque Inc.) with 5% KnockOut Serum Replacement (Thermo Fisher Scientific), and 1 μ g/mL doxycycline. The medium was changed every other day until the assay.

DYSF immunostaining. On day 7, each compound diluted in culture medium was added to the wells at final concentrations of 0.003 to 10 μ M. After 24 h treatment, cells were fixed by adding 4% paraformaldehyde (FUJIFILM Wako Pure Chemical Corporation) and incubated for 30 min. Cells were washed with PBS and blocked with 5% goat serum (Invitrogen Corp.) /0.4% TritonX-100 in PBS for 1 h at room temperature followed by the incubation with primary antibodies overnight at 4 °C. On the next day, cells were washed with PBS and incubated with secondary antibodies for 1 h at room temperature. Antibodies were diluted with PBS containing 1% goat serum and 0.4% TritonX-100, and Hoechst 33342 (DOJINDO LABORATORIES) was added to secondary antibody solution for nuclear staining. Stained cells were imaged by Opera

Phenix imaging system (PerkinElmer Japan Co., Ltd.). Dysferlin expression levels in differentiated myocyte were determined as the fluorescence intensity of 488 nm in dysferlin/MHC double positive area using Harmony software (PerkinElmer Japan Co., Ltd.).

Statistical analysis. The EC₁₅₀ value was defined as the concentration of the test compound required to produce 50% increase of dysferlin expression level. The signal value of the 100% control was obtained from the median value of DMSO treated wells. EC₁₅₀ values were calculated with XLfit (IDBS, Guildford, UK) using 4 parameter logistic models.

Aqueous Solubility Assay. Small volumes of the compound DMSO solutions were added to the aqueous buffer (pH 6.8). After incubation, precipitates were separated from by filtration through a filter plate. The filtrates were analyzed for compound in solution by plate reader or HPLC analysis.

Parallel Artificial Membrane Permeability Assay. The donor wells were filled with 200 μ L of PRISMA HT buffer (pH 7.4, Pion Inc.) containing 10 μ mol/L test compound. The filter on the bottom of each acceptor well was coated with 4 μ L of GIT-0 Lipid Solution (Pion Inc.) and filled

with 200 μL of Acceptor Sink Buffer (Pion Inc.). The acceptor filter plate was put on the donor plate and incubated for 3 hours at room temperature. After incubation, the amount of test compound in both the donor and acceptor wells was measured by LC/MS/MS.

Cytotoxicity Assay. HepG2 cells were cultured in DMEM high glucose medium (ThermoFisher Scientific, cat# 31053028) containing 2 mM L-glutamine, 1 mM sodium pyruvate, 5 mM HEPES, 10% (v/v) fetal bovine serum, 100 U ml^{-1} penicillin, and 100 $\mu\text{g ml}^{-1}$ streptomycin. The cells were seeded at 5000 cells/20 μL /well on 384-well plates (Greiner Bio-One, Frickenhausen, Germany) for nearly 24 h at 37 $^{\circ}\text{C}$ /5% CO_2 . Subsequently, 20 μL of the medium containing the test compounds were added to the plate, followed by 24 h of incubation at 37 $^{\circ}\text{C}$ /5% CO_2 . Subsequently, 20 μL of the Cell Titer Glo (Promega, Madison, WI) reagent was added to each well and the luminescence signal was measured using an EnVision plate reader. The signal values of the 0% and 100% inhibition controls were obtained from wells containing DMSO treated cells and the medium only, respectively. The percentage of inhibition was calculated using equation (1).

$$\% \text{ inhibition} = 100 \frac{\mu_H - T}{\mu_H - \mu_L} \quad (1)$$

1
2
3
4 , where T is the value of the wells containing test compounds, and μ_H and μ_L are the mean values
5
6
7 of the 0% and 100% inhibition control wells, respectively. IC_{50} values were calculated by fitting a
8
9
10 sigmoidal dose-response curve to the plot of the percentage of inhibition as a function of inhibitor
11
12
13 concentration. Fittings were performed using XLfit software (IDBS, Guildford, UK).
14
15
16
17
18
19
20

21 **Fluorescence Imaging of Tubulin Depolymerization.** HepG2 cells were seeded at 7500
22
23 cells/20 μ L/well on clear bottom 384-well plates (Corning, Corning, NY) in assay medium
24
25 (DMEM low glucose medium (Wako, Osaka, Japan) containing 10% FBS, 100 U mL^{-1}
26
27 penicillin, and 100 μ g mL^{-1} streptomycin). After incubation for nearly 24 h at 37 $^{\circ}C$ /5% CO_2 , 5
28
29
30 μ L of the assay medium containing 5 fold concentration of test compounds was added to each
31
32
33 well and the plate was further incubated for 24 h at 37 $^{\circ}C$ /5% CO_2 . To fix the cells, 25 μ L of 4%
34
35
36 paraformaldehyde phosphate buffer solution (Wako) was added into each well and the plate was
37
38
39 incubated for 30 min at room temperature. After removing the medium, the cells were washed
40
41
42 with PBS 3 times and 50 μ L of PBS-T (PBS containing 1.5% (w/v) BSA and 0.1% (v/v)
43
44
45 TritonX-100) was added to the plate for cell permeabilization and prevention of nonspecific
46
47
48 antibody binding. After 1 h incubation at room temperature, the plate was washed with PBS 3
49
50
51 times and the cells were incubated with 20 μ L of PBS-T containing 250 fold diluted
52
53
54
55
56

anti- α -tubulin antibody (TU-02) (ref#, sc-8035, Santa Cruz Biotechnology, Dallas, TX) followed by overnight incubation at 4 °C. After removing the solution, the cells were washed with PBS 3 times and 20 μ L of 12.5 μ M Hoechst 33342 (Thermo Fisher Scientific, Waltham, MA) and 400 fold diluted Alexa488-conjugated anti-mouse IgG antibody (ref#: A-11001, Thermo Fisher Scientific) in PBS-T containing was added to the plate. After 1 h incubation at room temperature, cells were washed 3 times and fluorescence images were obtained using an INCell Analyzer 6500 (GE Healthcare UK Ltd., Amersham Place, England) with a 20X objective lens. The fluorescence images were quantified using INCell Developer (GE Healthcare UK Ltd). In order to normalize the number of remaining cells in each well, fluorescence signal of Alexa488 (corresponding to tubulin) was corrected with number of nucleus stained with Hoechst 33342. Signals for 100% and 0% tubulin inhibition were obtained from the wells in the presence and absence of 2 μ M colchicine, respectively. Relative Alexa488 fluorescence intensity in the presence of each concentration of compounds was calculated by using equation (2).

$$\text{Relative intensity} = 100 \frac{T - \mu_L}{\mu_H - \mu_L} \quad (2)$$

, where T is the value of the wells containing test compounds, and μ_H and μ_L are the mean values of the 0% and 100% inhibition control wells, respectively. The dose-response curve was fitted with equation (3)

$$\text{Relative intensity} = \frac{100}{1 + 10^{n(\log[I] - \log IC_{50})}} \quad (3)$$

, where IC_{50} , $[I]$, and n are half maximal inhibitory concentration, concentration of test compounds and Hill slope, respectively. Minimal effective concentration (MEC) of each compound was calculated as the concentration where relative intensity corresponded to 100-3SD of 0% inhibition control wells by using equation (3). All fits were performed using XLfit software. The structure, EC_{150} value, and MEC value of tested compounds are shown in **Table S1**, Supporting Information.

Computational Methods and Modeling. The crystal structure of *sus barbatus* tubulin alpha chain/*gallus gallus* tubulin beta-2 chain dimer in complex with nocodazole (PDB code: 5CA1) was used as the template for docking. The identities of amino acids between human and *sus barbatus* for tubulin alpha chain and between human and *gallus gallus* for tubulin beta-2 chain are 99.5% and 99.1%, respectively. In addition, as all the amino acids within 6 Å of nocodazole are conserved between human and *sus barbatus* or *gallus gallus*, docking models with the structure of *sus barbatus* alpha and *gallus gallus* beta-2 tubulin dimer can be used to the interactions between human tubulin dimer and its inhibitor. The protein structure for docking was prepared using Maestro version 11.6 protein preparation wizard[X1]. The docking simulation was performed

with Glide version 7.9 SP mode[X2]. The top conformation in GlideScore was selected as the docking model.

[X1] Schrödinger Release 2018-2, Maestro, version 11.6, Schrödinger, LLC, New York, NY, 2018. [X2] Schrödinger Release 2018-2, Glide, version 7.9, Schrödinger, LLC, New York, NY, 2018.

Competitive Binding Assay with PAL probe.

Materials and Method. Following materials were used for photoaffinity labeling of α/β -tubulin: Porcine Tubulin (> 99% pure, Cytoskeleton, #T240); TAMRA-Azide (Tetramethylrhodamine 5-Carboxamido-(6-Azidoheptyl)), (Lifetechnologies, #T10182); Tris[(1-benzyl-1H-1,2,3-triazol-4-yl)methyl]amine (TBTA) (Tokyo Chemical Industry, #T2993); tert-butanol (t-BuOH) (SIGMA, #360538); Copper (II) Sulfate (SIGMA, #451657); Tris(2-carboxyethyl)phosphine (TCEP) (SIGMA, #C4706); low protein binding 96 well plate (Sumitomo Bakelite co. ltd., Proteosave #MS-8296V); Perfect NT Gel, 7.5-15%, 28 well (DRC, #NTH-787HP).

Experimental Procedure. Twenty five $\mu\text{g/mL}$ of tubulin in HEPES based isotonic buffer (20 mM HEPES, 140 mM NaCl, 10 mM KCl, 5% glycerol, pH 7.4), 196 μL , was mixed with 5 μL of DMSO or 1 - 10 mM compounds (compound **18**, compound **21**, nocodazole, vinblastine, colchicine, and paclitaxel) in DMSO for the competition study. The mixture was incubated for 30 min at room temperature, followed by addition of 2 μL of 0.01 mM PAL probe **28**, and incubated on ice for 15 min. The portion of this solution, 40 μL , was transferred to a low protein binding 96 well plate and irradiated by UV cross linker with CL-1000L lamp, 365 nm, 8W (UVP, Inc., #CL-100), for 5 min at 4 $^{\circ}\text{C}$. To the solution, 5 μL of 10% SDS, 1 μL of 5 mM TAMRA-Azide in DMSO, and 5 μL of catalyst mix for click-reaction (1.7 mM TBTA in 80% tert-butanol and 20% DMSO : 50 mM CuSO_4 : 50 mM TCEP = 3 : 1 : 1) were added and incubated for 1 h at room temperature: Catalyst mix was the prepared just before use. The obtained samples were mixed with Laemmli sample buffer including dithiothreitol (20 mM at the final concentration), and heated at 95 $^{\circ}\text{C}$ for 1 min, and 100 ng of tubulin for each condition was analyzed by SDS-PAGE (200 V, 50 min). The SDS-PAGE gel was scanned by Typhoon 9400 (Amersham Biosciences) to capture the image of PAL-probe-labeled tubulin, and stained by coomassie brilliant blue to observe the total tubulin, which were scanned by LAS4000 (Fujifilm).

SUPPORTING INFORMATION

The Supporting Information is available free of charge on the ACS Publications website at DOI:.

The structure, EC₁₅₀ value, and MEC value of compounds tested in the tubulin depolymerization assay; results of TR-FRET based competitive binding assays against 337 kinases (PDF)

Molecular formula strings. (CSV)

CORRESPONDING AUTHOR INFORMATION

Corresponding Author

*E-mail: hiroyuki.takada1@takeda.com. Phone: (+81)466-32-2076. Fax: (+81)466-29-4449.

AUTHORS' CONTRIBUTIONS

Author Contributions

The manuscript was written through contributions of all authors. All authors have given approval to the final version of the manuscript.

ACKNOWLEDGMENTS

We are grateful to Masanori Okaniwa, Tsuneo Oda, Yasuhisa Kohara, Mika Inoue, and Hiroshi

Imoto for their support to the synthesis study. We also thank Akiko Kume for the assistance with the dysferlin elevation assay. The kinase selectivity assay was carried out with the cooperation of Axcelead Drug Discovery Partners Inc.

ABBREVIATIONS USED:

AcOH, acetic acid; AcONH₄, ammonium acetate; BSA, bovine serum albumin; DIPEA, *N,N*-diisopropylethylamine; DMAT, distal myopathy with anterior tibial onset; DME, 1,2-dimethoxyethane; DMF, dimethylformamide; DMSO-*d*₆, deuterated dimethyl sulfoxide; EtOAc, ethyl acetate; HATU, 2-(7-aza-1*H*-benzotriazole-1-yl)-1,1,3,3-tetramethyluronium hexafluorophosphate; iPSC, induced pluripotent stem cell; LGMD2B, limb girdle muscular dystrophy 2B; MeCN, acetonitrile; MEC, minimal effective concentration; MM, Miyoshi myopathy; PAL, photoaffinity labeling; PBS, phosphate buffered salts; Pd(Amphos)Cl₂, bis(di-*tert*-butyl(4-dimethylaminophenyl)phosphine)dichloropalladium(II); PdCl₂(PPh₃)₂, bis(triphenylphosphine)dichloropalladium(II); PdCl₂(dppf), [1,1'-bis(diphenylphosphino)ferrocene]dichloropalladium(II); Pd(PPh₃)₄, tetrakis(triphenylphosphine)palladium(0); SAR, structure-activity relationships; TAMRA, tetramethylrhodamine; TFA, trifluoroacetic acid; THF, tetrahydrofuran.

REFERENCES

1. Swinney, D. C.; Anthony, J. How were new medicines discovered? *Nat Rev Drug Discov* **2011**, 10, 507-519.
2. Moffat, J. G.; Vincent, F.; Lee, J. A.; Eder, J.; Prunotto, M. Opportunities and challenges in phenotypic drug discovery: an industry perspective. *Nat Rev Drug Discov* **2017**, 16, 531-543.
3. Heilker, R.; Traub, S.; Reinhardt, P.; Scholer, H. R.; Sternecker, J. iPS cell derived neuronal cells for drug discovery. *Trends Pharmacol Sci* **2014**, 35, 510-519.
4. Vincent, F.; Loria, P.; Pregel, M.; Stanton, R.; Kitching, L.; Nocka, K.; Doyonnas, R.; Stepan, C.; Gilbert, A.; Schroeter, T.; Peakman, M. C. Developing predictive assays: the phenotypic screening "rule of 3". *Sci Transl Med* **2015**, 7, 293ps15.
5. Imamura, K.; Izumi, Y.; Watanabe, A.; Tsukita, K.; Woltjen, K.; Yamamoto, T.; Hotta, A.; Kondo, T.; Kitaoka, S.; Ohta, A.; Tanaka, A.; Watanabe, D.; Morita, M.; Takuma, H.; Tamaoka, A.; Kunath, T.; Wray, S.; Furuya, H.; Era, T.; Makioka, K.; Okamoto, K.; Fujisawa, T.; Nishitoh, H.; Homma, K.; Ichijo, H.; Julien, J. P.; Obata, N.; Hosokawa, M.; Akiyama, H.; Kaneko, S.; Ayaki, T.; Ito, H.; Kaji, R.; Takahashi, R.; Yamanaka, S.; Inoue, H. The Src/c-Abl

pathway is a potential therapeutic target in amyotrophic lateral sclerosis. *Sci Transl Med* **2017**, 9, eaaf3962.

6. Hino, K.; Horigome, K.; Nishio, M.; Komura, S.; Nagata, S.; Zhao, C.; Jin, Y.; Kawakami, K.; Yamada, Y.; Ohta, A.; Toguchida, J.; Ikeya, M. Activin-A enhances mTOR signaling to promote aberrant chondrogenesis in fibrodysplasia ossificans progressiva. *J Clin Invest* **2017**, 127, 3339-3352.

7. Liu, J.; Aoki, M.; Illa, I.; Wu, C.; Fardeau, M.; Angelini, C.; Serrano, C.; Urtizberea, J. A.; Hentati, F.; Hamida, M. B.; Bohlega, S.; Culper, E. J.; Amato, A. A.; Bossie, K.; Oeltjen, J.; Bejaoui, K.; McKenna-Yasek, D.; Hosler, B. A.; Schurr, E.; Arahata, K.; de Jong, P. J.; Brown, R. H., Jr. Dysferlin, a novel skeletal muscle gene, is mutated in Miyoshi myopathy and limb girdle muscular dystrophy. *Nat Genet* **1998**, 20, 31-36.

8. Bashir, R.; Britton, S.; Strachan, T.; Keers, S.; Vafiadaki, E.; Lako, M.; Richard, I.; Marchand, S.; Bourg, N.; Argov, Z.; Sadeh, M.; Mahjneh, I.; Marconi, G.; Passos-Bueno, M. R.; Moreira Ede, S.; Zatz, M.; Beckmann, J. S.; Bushby, K. A gene related to *Caenorhabditis elegans* spermatogenesis factor *fer-1* is mutated in limb-girdle muscular dystrophy type 2B. *Nat Genet* **1998**, 20, 37-42.

9. Anderson, L. V.; Davison, K.; Moss, J. A.; Young, C.; Cullen, M. J.; Walsh, J.; Johnson, M. A.; Bashir, R.; Britton, S.; Keers, S.; Argov, Z.; Mahjneh, I.; Fougere, F.; Beckmann, J. S.; Bushby, K. M. Dysferlin is a plasma membrane protein and is expressed early in human development. *Hum Mol Genet* **1999**, 8, 855-861.
10. Bansal, D.; Campbell, K. P. Dysferlin and the plasma membrane repair in muscular dystrophy. *Trends Cell Biol* **2004**, 14, 206-213.
11. Han, R. Muscle membrane repair and inflammatory attack in dysferlinopathy. *Skeletal Muscle* **2011**, 1, 10.
12. Matsuda, C.; Kiyosue, K.; Nishino, I.; Goto, Y.; Hayashi, Y. K. Dysferlinopathy fibroblasts are defective in plasma membrane repair. *PLoS Curr* **2015**, 7. DOI: 10.1371/currents.md.5865add2d766f39a0e0411d38a7ba09c.
13. Takahashi, T.; Aoki, M.; Suzuki, N.; Tateyama, M.; Yaginuma, C.; Sato, H.; Hayasaka, M.; Sugawara, H.; Ito, M.; Abe-Kondo, E.; Shimakura, N.; Ibi, T.; Kuru, S.; Wakayama, T.; Sobue, G.; Fujii, N.; Saito, T.; Matsumura, T.; Funakawa, I.; Mukai, E.; Kawanami, T.; Morita, M.; Yamazaki, M.; Hasegawa, T.; Shimizu, J.; Tsuji, S.; Kuzuhara, S.; Tanaka, H.; Yoshioka,

M.; Konno, H.; Onodera, H.; Itoyama, Y. Clinical features and a mutation with late onset of limb girdle muscular dystrophy 2B. *J Neurol Neurosurg Psychiatry* **2013**, 84, 433-440.

14. Tanaka, A.; Woltjen, K.; Miyake, K.; Hotta, A.; Ikeya, M.; Yamamoto, T.; Nishino, T.; Shoji, E.; Sehara-Fujisawa, A.; Manabe, Y.; Fujii, N.; Hanaoka, K.; Era, T.; Yamashita, S.; Isobe, K.; Kimura, E.; Sakurai, H. Efficient and reproducible myogenic differentiation from human iPS cells: prospects for modeling Miyoshi myopathy in vitro. *PLoS One* **2013**, 8, e61540.

15. Kokubu, Y.; Nagino, T.; Sasa, K.; Oikawa, T.; Miyake, K.; Kume, A.; Fukuda, M.; Fuse, H.; Tozawa, R.; Sakurai, H. Phenotypic drug screening for dysferlinopathy using patient-derived induced pluripotent stem cells. *Stem Cells Transl Medicine* **2019**, *in press*. DOI: 10.1002/sctm.18-0280

16. Oda, T.; Imada, T.; Naito, K.; Tamura, T.; Furuya, S. Bicyclic Derivative, Process for Producing the Same, and Use. *PCT Int. Appl.* **2003**, WO 03/045929 A1.

17. Ziegler, S.; Pries, V.; Hedberg, C.; Waldmann, H. Target identification for small bioactive molecules: finding the needle in the haystack. *Angew Chem Int Ed Engl* **2013**, 52, 2744-2792.

18. Comess, K. M.; McLoughlin, S. M.; Oyer, J. A.; Richardson, P. L.; Stockmann, H.; Vasudevan, A.; Warder, S. E. Emerging approaches for the identification of protein targets of small molecules - a practitioners' perspective. *J Med Chem* **2018**, 61, 8504-8535.
19. Lu, Y.; Chen, J.; Xiao, M.; Li, W.; Miller, D. D. An overview of tubulin inhibitors that interact with the colchicine binding site. *Pharm Res* **2012**, 29, 2943-2971.
20. Wang, Y.; Zhang, H.; Gigant, B.; Yu, Y.; Wu, Y.; Chen, X.; Lai, Q.; Yang, Z.; Chen, Q.; Yang, J. Structures of a diverse set of colchicine binding site inhibitors in complex with tubulin provide a rationale for drug discovery. *FEBS J* **2016**, 283, 102-111.
21. Murale, D. P.; Hong, S. C.; Haque, M. M.; Lee, J. S. Photo-affinity labeling (PAL) in chemical proteomics: a handy tool to investigate protein-protein interactions (PPIs). *Proteome Sci* **2016**, 15, 14.
22. Dominguez-Brauer, C.; Thu, K. L.; Mason, J. M.; Blaser, H.; Bray, M. R.; Mak, T. W. Targeting mitosis in cancer: emerging strategies. *Mol Cell* **2015**, 60, 524-536.
23. Okita, K.; Yamakawa, T.; Matsumura, Y.; Sato, Y.; Amano, N.; Watanabe, A.; Goshima, N.; Yamanaka, S. An efficient nonviral method to generate integration-free human-induced pluripotent stem cells from cord blood and peripheral blood cells. *Stem Cells* **2013**, 31, 458-466.

24. Nakagawa, M.; Taniguchi, Y.; Senda, S.; Takizawa, N.; Ichisaka, T.; Asano, K.; Morizane, A.; Doi, D.; Takahashi, J.; Nishizawa, M.; Yoshida, Y.; Toyoda, T.; Osafune, K.; Sekiguchi, K.; Yamanaka, S. A novel efficient feeder-free culture system for the derivation of human induced pluripotent stem cells. *Sci Rep* **2014**, 4, 3594.

25. Uchimura, T.; Otomo, J.; Sato, M.; Sakurai, H. A human iPS cell myogenic differentiation system permitting high-throughput drug screening. *Stem Cell Res* **2017**, 25, 98-106.

Table of Contents graphic

